

Republic of Iraq

Ministry of Higher Education & Scientific Research

Al-Nahrain University

College of Science



Image Restoration Using Adaptive Nonlinear Techniques

A Thesis

Submitted to the College of Science of Al-Nahrain University as a
Partial Fulfillment of the Requirements for the Degree of Master of
Science in Physics

By

Mohammed Khudier Kadhom

(B.Sc. 2005)

Supervised by

Professor Dr. Ayad A. Al-Ani

Assistant Professor Dr. Salah A. Saleh

Rabi' Thani.

1429

April

2008

بِسْمِ اللَّهِ الرَّحْمَنِ الرَّحِيمِ

وَقُلْ اَعْمَلُوا فَسَيَرَى اللَّهُ عَمَلَكُمْ وَرَسُولُهُ وَالْمُؤْمِنُونَ

وَسَتُرَدُّونَ اِلَى عَالَمِ الْغَيْبِ وَالشَّهَادَةِ فَيُنَبِّئُكُمْ بِمَا

كُنْتُمْ تَعْمَلُونَ

صدق الله العظيم

(التوبة: ١٠٥)

List of Contents

Certification

Acknowledgment

Abstract

page

Chapter One: General Introduction

1.1	Introduction	1
1.2	Historical Survey	3
1.3	Aim of the Thesis	6
1.4	Thesis Layouts	6

Chapter Two: Image Model and Image Manipulation

2.1	Introduction	8
2.2	Image Formation	9
2.2.1	Blur Model (point spread function)	10
	• Space - Invariant Point Spread Function (SIPSF)	11
	• Space -Variant Point Spread Function (SVPSF)	11
a.	Atmospheric turbulence blur (Gaussian blur)	11
b.	Motion Blur	12
c.	Uniform Out Of Focus Blur	13
2.3	Noise Model	14
a.	Additive Noise	18
b.	Multiplicative Noise	18
2.4	Image Restoration	19
2.4.1	Image Restoration Algorithms	19
I.	Frequency Domain Filters	20

1. Inverse Filter	20
2. Wiener Filter	21
3. Constrained Least-Squares Filter	23
II. Iterative image restoration algorithms	24
3.5 Image Quality	28

Chapter Three: Results and Discussion

3.1 Introduction	32
3.2 Practical Part	33
Image Restoration Algorithm	33
3.3 Results	35
3.4 Results discussion	74

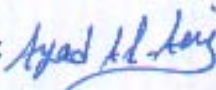
Chapter Four: Conclusions and Future Work


4.1 Conclusions	77
4.2 Suggest For Future Work	77

<i>References</i>	78
--------------------------	----

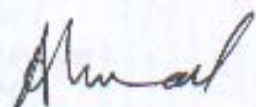
CERTIFICATION

We certify that this thesis entitled "**Image Restoration Using Adaptive Nonlinear Techniques**" was prepared by "**Mr. Mohammed Khudier Kadhom**" under our supervision at College of Science, Al-Nahrain University as a partial fulfillment of the requirements for the degree of **Master of Science in Physics**.

Signature: 
Name : **Dr. Ayad A. Al-Ani**
Title : **Professor**
Date : / / **2008**


Signature: 
Name : **Dr. Salah A. Saleh**
Title : **Assistant Professor**
Date : / / **2008**

In view of the available recommendations, I forward this thesis for debate by the examination committee.

Signature: 
Name : **Dr. Ahmad. K. Ahmad**
Title : **Assistant Professor**
Address: **Head of Department of Physics**
Date : / / **2008**


Examination Committee Certification

We certify that we have read the thesis entitled " *Image Restoration Using Adaptive Nonlinear Techniques* " and as an examination committee, examined the student **Mr. Mohammed Khudier Kadhom** on its contents, and that in our opinion it is adequate for the partial fulfillment of the requirements of the degree of **Master of Science in Physics**.

Signature: 


Name: **Dr. Kais J. Latif**
Title: **Assistant Professor**
(Chairman)

Date: 30 / 6 / 2007

Signature: 

Name: **Dr. Ali A. D. Al-Zuky**
Title: **Assistant Professor**
(Member)

Date: 7 / 7 / 2007

Signature: 

Name: **Dr. Sawsan Kamal Thamer**
Title: **Lecturer**
(Member)

Date: 30 / 6 / 2007

Signature: 

Name: **Dr. Ayad A. Al-Ani**
Title: **Professor**
(Supervisor)

Date: 15 / 7 / 2007

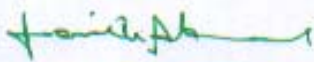
Signature: 

Name: **Dr. Salah A. Saleh**
Title: **Assistant Professor**
(Supervisor)

Date: / / 2007

Approved by the College Committee of Postgraduate studies



Signature: 

Name: **Dr. LAITH ABDUL AZIZ AL- ANI**
Title: **Assistant Professor**
(Dean of the College of Science)

Date: 11 / 7 / 2007

Acknowledgments

Thanks to our GOD the most merciful and gracious for enabling me to complete this thesis.

I would like to express my sincere thanks and deep gratitude to my supervisors *Professor Dr. Ayad A. Al-Ani* and *Assistant Professor Dr. Salah A. Saleh* for supervising the present work and for their support, encouragement and suggestions throughout the work.

Special thanks and deep affection to my family, and my wife for their love, help, and supports through the years.

Finally, I would like to extend my thanks and gratitude to all who had ever assisted me during the period of this research.

Mohammed Khudier

Abstract

Image restoration is the process of finding an approximation to the degradation process and find appropriate inverse process to estimate the original image.

An iterative restoration technique(Tikhonov method) was adapted. The adapted filter was designed for restoring RGB satellite images that are blurred with space-invariant point spread function, Gaussian function, and corrupted with additive noise, and salt & pepper noise. Different degradation parameters, i.e. different signal to noise ratio were considered and different noise density.

The results using an adaptive filter were compared, quantitatively, with different types of conventional restoration techniques, (such as inverse filter, Least-Squares filter (Wiener Filter), and Constrained Least-Squares filter) using Mean Square Error (MSE). Results show that The Mean Square Error of the restored images decreases with increasing the number of iteration until the result convergence. Also the ratio of the MSE of the degraded image to the restored image will increase with decreasing SNR for Gaussian noise, and with increasing noise density for salt and pepper noise respectively, then Results show this method has better performance for restoring the degraded images, especially for low signal to noise ratio, and for high noise density.



CHAPTER ONE



General Introduction

1.1 General Introduction

The term digital has become part of our daily lives. It derives from Latin *digitus*, finger, and has since then quite understandably come to mean 'numerical' or 'number-related'. The word is known from constructs such as 'digital clock' (a clock showing time as numbers or digits); even 'digital sound' is a well-known concept today [1].

The field of digital image processing has a quite long history in astronomy that began in the 1950's with the space program. The first images of Moon (mainly of the opposite side), at that time of unimaginable resolution. However, the images were obtained under big technical difficulties such as vibrations, motion due spinning, etc. The need to retrieve as much information as possible from such degraded images was the aim of the early efforts to adapt the one-dimensional signal processing algorithms to images, creating a new field that is today known as "Digital Image Processing" [2].

The techniques of image reconstruction and restoration have been a "must" in all scientific disciplines involving projections or interferometer data. However, for a long time image processing was considered as a luxury in other fields such as optical astronomy. It also applied to image coming from space [3].

The term digital image processing generally refers to processing of a two-dimensional picture by a digital computer [4].

Interest in digital image processing methods stems from two principal application areas: improvement of pictorial information for human interpretation. And processing of scene data for autonomous machine perception [5].

Digital image processing has a broad spectrum of applications, such as remote sensing via satellites and other spacecrafts, image transmission and storage for business applications, medical processing,

radar, sonar, and acoustic image processing, robotics, and automated inspection of industrial parts [4].

Typical problems in machine perception that routinely employ image processing techniques are automatic character recognition, industrial robots for product assembly and inspection, military recognizance, automatic processing of fingerprints, screening of x-rays and blood samples, and machine processing of aerial and satellite imager for weather prediction and crop assessment [5].

Image restoration is the process of taking an image with some known, or estimated degradation, the restoring it to its original appearance, Image restoration often used in the field of photography or publishing where an image was somehow degraded but needs to be improved before it can be printed. For this type of application, know are needed to something about the degradation process in order to develop model for the distortion. When a model for the degradation process has, the inverse process can be applied to the image to restore it to its original form [6].

There are no techniques so far, that can produce a perfect restoration or that can be recommend for use in each and every case of degradation. In order to choose or to design a method of image restoration it is necessary and very important to characterize the degradation effect and also some prior information about the degraded image [7].

1.2 Historical Survey

Detailed discussion of the earlier developments in restoration techniques can be found in Sondi, Andrews, Hunt, Rosenfeld and Kak, Bates et. al., Gonzalz and Wintz , Sezan & Tekalp. Unfortunately, the book by Andrews and Hunt, published in 1977 is the only available book specialized in the field of image restoration [8].

In fact, a variety of digital techniques has been proposed and developed for the enhancement or restoration considering the recovering of original images from degraded images. However, it can be seen from the published literature that a number of image restoration techniques have been derived from linear filtering [9]. One basic approach for stochastic methods is to use the Wiener filter in the frequency domain and then linear restoration filter in the spatial domain [10].

In the past few years there has been great interest in the development of recursive filtering techniques for time domain signals. These techniques have been recently applied to image restoration [8] with the hope of alleviating the high computational burden and obtaining optimal restoration [10].

In 1987, Denise, and Howard [11] were developed color image restoration, taking into account the correlation between color components.

In 1999, Geert and Lucas [12] were studied the essential difference of non-linear image restoration algorithms with linear image restoration filter is their capability to restrict the restoration result to non-negative intensities. The Iterative Constrained Tikhnov-Miller algorithm (ICTM) algorithms. They are showed that this dramatically deteriorate the performance of the non-linear restoration algorithms. And they are proposing a novel method to estimate the background based on the dependency of non-linear restoration algorithms on the background.

In 2000, Geert and Lucas [13] were studied on the influence of the regularization parameter and the first estimate on the performance of iterative image restoration algorithms. They were discussed regularization parameter estimation methods that have been developed for the linear Tikhonov – Miller filter to restore images distorted by additive Gaussian noise; they found that most algorithms converged for most choices.

In 2003, Hao and his college [14] were presented a new technique for acceleration of iterative image restoration algorithms, unlike other fast algorithms which tend to accelerate the rate of convergence of iterative procedure.

In 2003, Sang and his college [15] were introduced the regularization method to suppress over-amplification. However, the regularization causes the reblurring problem and does not eliminate ringing artifacts effectively. A directional regularization approach is proposed to reduce the reblurring problem and the ringing artifacts in iterative image restoration.

In 2004, Stuart *at el.* [16] were developed a novel, perceptually inspired image restoration method which takes human perception knowledge into consideration to reverse the effect blur; they have been show that the new restoration algorithm visually restores images as well as the previously presented LVMSE-based algorithm.

In 2005, Yuk and Yik [17] were studied the restoration of color-quantized images, they are proposed a restoration algorithm for restoring color-quantized images, simulation results show that it can improve the quality of a color –quantized image remarkably in terms of both SNR and CIELAB color difference metric.

In 2006, Feng *at el.* [18] were presented a new iterative regularization algorithm. Before restoration, they have been divided the pixels of the blurred and noisy image into two types of regions: flat

region and edge region (edge and the regions near edge), and they are showed that algorithm is effective and the edge details are well preserved during the restoration process.

In 2006, Paola *at el.* [19] were studied in many image restoration applications the nonnegative of the computed solution is required. General regularization methods, such as iterative semi convergent methods, seldom compute nonnegative solutions even when the data are nonnegative. Some methods can be modified in order to enforce the nonnegative constraint.

In 2006, Ayad A. Al-ani [20] was adapted in many image restorations an iterative Wiener filter. To estimate the power spectral density of the original image from degraded image using an iterative method. The adapted filter was designed for restoring astronomical images that are blurred with space-invariant point spread function and corrupted with additive noise .the result using an adaptive filter were compared, quantitatively, using mean square error (MSE).His result shows that this method has better performance for restoring the degraded images, especially for high signal to noise ratio.

In 2007,Tony and his college [21] were discussed studied many variant ional models for image denoising restoration are formulated in primal variables that are directly linked to the solution to be restored ,they are proposed a linearized primal dual iterative method as an alternative stand-alone approach to solve the dual formulation without regularization. Numerical results are presented to show that the proposed methods are much faster than the Chambolle method.

In 2007, Wenyi and his college [22] were discussed the task of deblurring, a form of image restoration, is to recover an image form its blurred version. Whereas most existing methods assume a small amount of additive noise, image restoration under significant additive noise

remains an interesting research problem. They are described two techniques to improve the noise handling characteristics of a recently proposed variational framework for semi-blind image deblurring that is based on joint segmentation and deblurring. One technique uses a structure tensor as a robust edge- indicating function. The other uses nonlocal image averaging to suppress noise. They are reported promising results with these techniques for the case of a known kernel.

1.3 Aim of the thesis

The aim of this thesis is to restore a degraded image, which blurred by Gaussian function and corrupted by an additive white noise, and salt and pepper noise using non linear method.

The adaptive technique is solved by estimating the power spectral density of the original image" object" from the degraded image. The adaptive technique (Tikhonov method) is compared with different types of conventional restoration techniques (Inverse filter, Least-Square filter (Weiner filter), constrained Least-Square filter (Regular filter)).

The aim of comparative study shows is one method better than other.

1.4 Thesis Layout

This thesis is organized as follows:

- Chapter one, presents a general introduction of image processing.
- Chapter two, deals with general background on the image formation, and described the most important methods and filters for image restoration and the parameters that effect the image quality and the most important image quality function.

- Chapter three, describes the computer simulation models which restore image by using (inverse filter, least Least-Squares Filter (wiener Filter), and Constrained Least-Squares Filter (Regular Filter, Tikhonov filter).
- Chapter four contains the conclusions of this work and suggestion for future work.



CHAPTER TWO

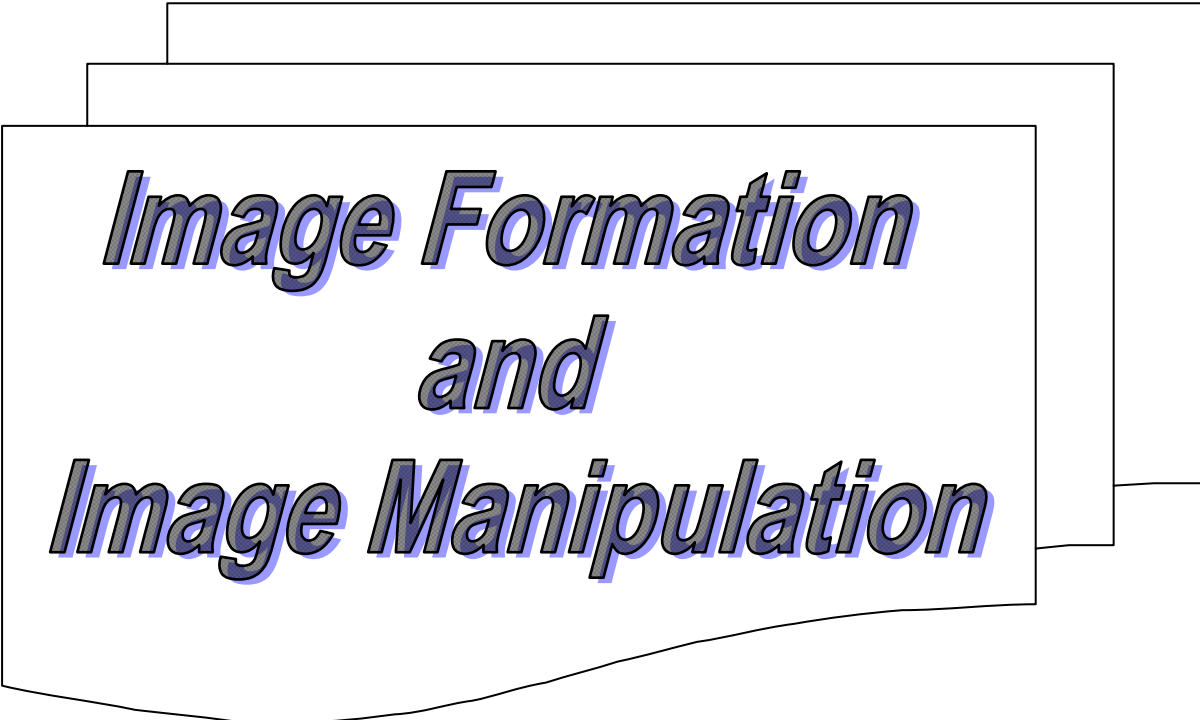


*Image Formation
and
Image Manipulation*

2.1 Introduction

When light is reflected by emitted from an object, it travels to the image plane through a medium which is not always homogenous. the inhomogeneous of the medium produces some degree of distortion. The source of distortion will be illustrated later in this chapter. This source includes the blur and noise function. The blur function has two types these are space variant and space invariant. The motion blur which is one of blur function that is resulting from a motion of imaging system or the object through the imaging period , atmospheric turbulence blur is another type of blur model, aberration is another type of blur model, and uniform out-of-focus is another type of blur model.

The ultimate goal of restoration techniques, however, is to improve a given image in some sense. It is therefore, an attempt to reconstruct or recover an image that has been degraded, using some a prior knowledge of the degradation phenomenon [5].

Generally, image formation processes can be described with a small number of equivalent physical concepts and an associated set of equation. There are many algorithms developed to overcome the problem of image restoration; e.g. linear and nonlinear, iterative and non-iterative, recursive and non- recursive, generalized algorithms and specialized algorithms. Some of these are applied in frequency domain while others in spatial domain.

Image quality is the another subject in this chapter. Image quality gives a criterion to show the degree of distortion between the reference images and the degraded one of the same scene [3].

2.2 Image Formation

The term image simply, refers to a two-dimensional light intensity function " $g(x,y)$ ", where x and y denote spatial coordinates and the value of g at any point (x,y) is proportional to the brightness (or gray level) of the image at that point [5].

light is a form of energy, must be nonzero and finite; i.e. [5]:

$$0 < g(x,y) < \infty \quad (2-1)$$

The basic nature of $g(x,y)$ may be characterized by two components [6]:

- 1 - The amount of source light incident on the scene being viewed.
- 2- The amount of light reflected by the objects in the scene.

Appropriately, they are called the illumination and reflectance components, and are denoted by $i(x,y)$ and $r(x,y)$, respectively. The function $i(x,y)$ and $r(x,y)$ combine as product to form $g(x,y)$ [5]:

$$g(x,y) = i(x,y) r(x,y) \quad (2-2)$$

where

$$0 < i(x,y) < \infty \quad (2-3)$$

and

$$0 < r(x,y) < 1 \quad (2-4)$$

Equation (2-4) indicates that reflectance is bounded by 0 (total absorption) and 1 (total reflectance). The nature of $i(x,y)$ is determined by the light source, and $r(x,y)$ is determined by the characteristics of the object in a scene [6].

The degradation process model consists of two parts, the degradation function and the noise function. The general model in the spatial domain follows [6]:

$$g(x, y) = h(x, y) \otimes f(x, y) + n(x, y) \quad (2-5)$$

where

\otimes denotes the convolution process

$g(x,y)$ degraded image

$h(x,y)$ degradation function, which is called point spread function (psf).

$f(x,y)$ original image

$n(x,y)$ additive noise function.

The Fourier Transform of eq. (2-5) is given by:

$$G(u, v) = H(u, v)F(u, v) + N(u, v) \quad (2-6)$$

$G(u,v)$ = Fourier transform of the degraded image.

$H(u,v)$ = Fourier transform of the degraded function.

$F(u,v)$ = Fourier transform of the original image.

$N(u,v)$ = Fourier transform of the additive noise function.

$H(u,v)$ is called the forward transfer function of the process. The inverse transform of the system transfer function, is called the impulse response in the terminology of linear system theory. $H(u,v)$ is called optical transfer function, and its magnitude is called the Modulation Transfer Function [5].

2.2 .1 Blur Model point spread function

It represents the most operative image degradation. It determines the energy distribution in the image plane due to point source located on the object plane [3].

Blur model can categorized into two types [3]:

1-Space-Invariant Point Spread Function (SIPSF).

2-Space-Variant Point Spread Function (SVPSF).

1. Space-Invariant Point Spread Function (SIPSF)

The point source explores the object plane, the point spread function changes only the position of the input but merely changes the location of the output with keeping the same function, This characteristic appears in the linear system. For example, the most optical telescope and microscope.

Thus the final image can be represented by a convolution process with ideal image $f(x_0, y_0)$:

$$g(x, y) = \int_{-\infty}^{+\infty} \int f(x_0, y_0) h(x - x_0, y - y_0) dx_0 dy_0 + n(x, y) \quad (2-7)$$

Where (x_a, y_0) and (x, y) represent the coordinates of the object and image form respectively[9].

2. Space-Variant Point Spread Function (SVPSF).

This type changes shape as well as position, i.e. the point spread function depends on the location of the object ,this property associated with nonlinear system [3].

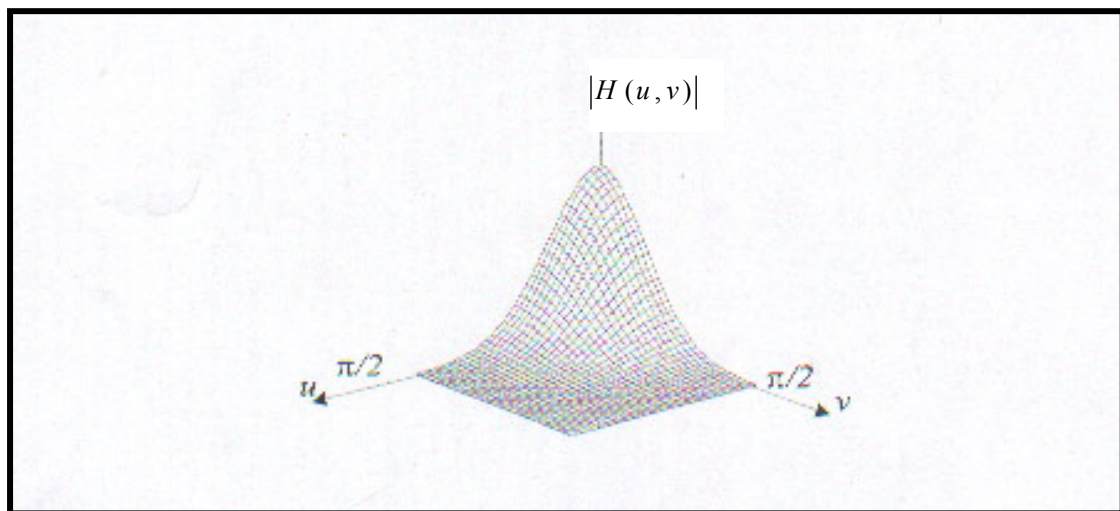
a. Atmospheric turbulence blur

Atmospheric turbulence is severe limitation in Astronomy, remote sensing and aerial imaging as used for example weather predictions. Though the blur introduced by atmospheric turbulence depends on a variety of factors (such as temperature, wind speed, exposure time), for long term exposures the PSF can reasonably well be described by a Gaussian function[23]:

$$h(x, y, \sigma) = C \exp\left(-\frac{x^2 + y^2}{2\sigma^2}\right) \quad (2-8)$$

Here σ determines the severity of the blur. C is constant depends on the type of turbulence which is usually found experimentally [24].

Figure(2-1) shows Gaussian blur in the Fourier domain:



Figure(2-1) Gaussian blur in the Fourier domain [23].

b. Motion Blur

Many types of motion blur can be distinguished, all of which are due to relative motion between the recording device and the scene. This can be in the form of a translation, a rotation, a sudden change of scale, or some combinations of these. Here only the important case of a global translation will be considered[23].

When the object translates at a constant velocity V under an angle of ϕ radians with the horizontal axis during the exposure interval $[0, T]$, then blurring function is given by [23]:

$$h(x, y, L, \phi) = \begin{cases} \frac{1}{L} & \text{if } \sqrt{x^2 + y^2} \leq \frac{L}{2} \leq \frac{x}{y} = -\tan \phi \\ 0 & \text{elsewhere} \end{cases} \quad (2-9)$$

The discrete version of eq. (2-9) is not easily captured in a closed form expression in general. For the special case that $\phi = 0$, an appropriate approximation eq. (2-9) is given by [23]:

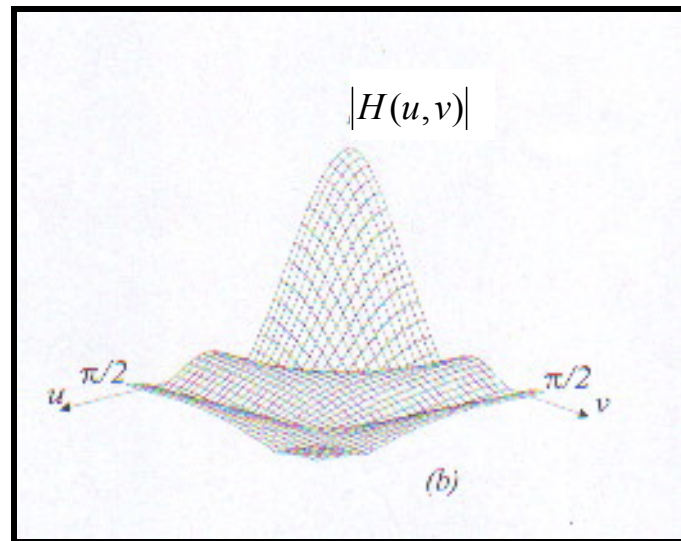
$$h(x, y, L, \phi) = \begin{cases} \frac{1}{L} & \text{if } x_1 = 0, |x_2| \leq \left[\frac{L-1}{2} \right] \\ \frac{1}{2L} \left\{ (L-1) - 2 \left[\frac{L-1}{2} \right] \right\} & \text{if } x_1 = 0, |x_2| = \left[\frac{L-1}{2} \right] \\ 0 & \text{elsewhere} \end{cases} \quad (2-10)$$

c. Uniform Out-Of-Focus Blur

When a camera images a 3-D scene onto a 2-D imaging plane, some parts of the scene are in focus while other parts are not. If the aperture of the camera is circular, the image of any point source is a small disk, known as the Circle Of Confusion (COC). The degree of defocus (diameter of the COC) depends on the focal length, the aperture number of the lens, and the distance between camera and object. An accurate model not only describes the diameter of the COC, but also the intensity distribution within the COC. The spatially continuous PSF of this uniform out-of-focus blur with radius R is given by [23]:

$$h(x, y, R) = \begin{cases} \frac{1}{\pi R^2} & \text{if } \sqrt{x^2 + y^2} \leq R \\ 0 & \text{elsewhere} \end{cases} \quad (2-11)$$

Figure(2-2) shows PSF in the Fourier domain of uniform out of focus Blur:



Figure(2-2):PSF in the Fourier domain
(Uniform Out-Of-Focus Blur) [23].

2.3 Noise Model

Noise is any undesired information that contaminates an image [6]. Or, they are random background events which have to be dealt with in every system processing real signals. They are not part of the ideal signal and may be caused by a wide range of sources, e.g. variations in the detector sensitivity, environmental variations, the discrete nature of radiation, transmission or quantization errors, etc [4].

The noise can be modeled with either a Gaussian (normal), uniform, or salt-and-pepper (impulse) distribution. The shape of the distribution of these noise types as a function of gray level can be modeled as a histogram.

Gaussian noise distribution which can be analytically described by [6]:

$$P(g) = \frac{1}{\sqrt{2\pi\sigma^2}} e^{-\frac{(g-m)^2}{2\sigma^2}} \quad (2-12)$$

where:

g = gray level

m = mean (average)

σ^2 = variance of the noise.

The uniform distribution which is given by [6]:

$$P(g) = \begin{cases} \frac{1}{b-a} & \text{For } a \leq g \leq b \\ 0 & \text{elsewhere} \end{cases} \quad (2-13)$$

where

$$\text{mean} = \frac{a+b}{2}$$

$$\text{variance} = \frac{(b-a)^2}{12}$$

With the uniform distribution, the gray level values of the noise are evenly distributed across a specific range [6].

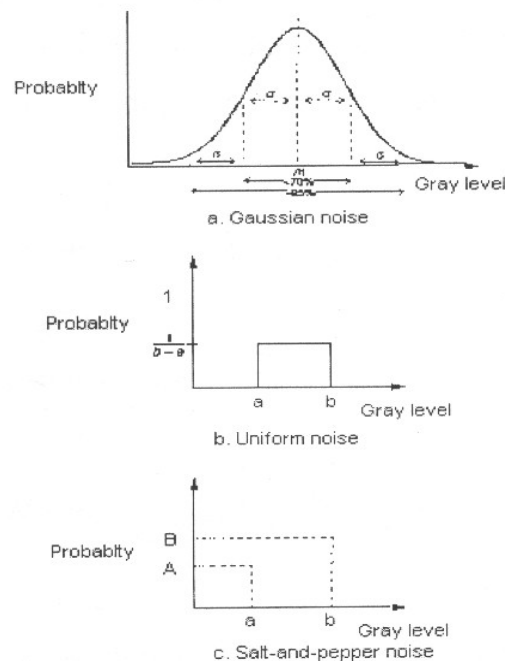
The salt-and-pepper distribution is given by:

$$P(g)_{\text{salt-and-pepper}} = \begin{cases} A & \text{For } g=a \text{ ("pepper")} \\ B & \text{For } g=b \text{ ("salt")} \end{cases} \quad (2-14)$$

In the salt-and-pepper noise model there are only two possible values, a and b , and the probability of each is typically less than 0.1-with number greater than this,. For 8-bit image, the typical value for pepper noise is 0 and for salt is 255[6].

The Gaussian model is most often used to model natural noise processes, such as those occurring from electronic noise in the image acquisition system. The salt-and-pepper type noise is typical caused by malfunctioning pixel elements in the camera sensor, faulty memory locations, or timing error in the digitization process. Uniform is useful because it can be used to general any other type of noise distribution and is often used to degrade image for the evaluation of image restoration algorithms because it provides the most unbiased or a neutral noise model [6].

Figure (2-3a) shows the Gaussian noise distribution, Figure (2-3b) shows the uniform noise distribution, and Figure(2-3c) shows the salt and pepper noise distribution,



Fig(2-3) Noise distribution [6].

In addition to the Gaussian, other noise models based on exponential distributions are useful for modeling noise in certain type of digital images. Radar range and velocity images typically contain noise that can be modeled by the Raleigh distribution, defined by [6]:

$$P(g) = \frac{2g}{\alpha} e^{-g^2/\alpha} \quad (2-15)$$

where :

$$mean = \sqrt{\frac{\pi\alpha}{4}}$$

$$variance = \frac{\alpha(4 - \pi)}{4}$$

The peak value for the Raleigh distribution is at $\sqrt{\alpha/2}$

Negative exponential noise occurs in laser-based images, and if this type of image is low pass filtered, the noise can be modeled as gamma noise. the equation for the negative exponential noise.

$$P(g)_{Negative-Exponential} = \frac{e^{-g^2/\alpha}}{\alpha} \quad (2-16)$$

Where variance $=\alpha^2$

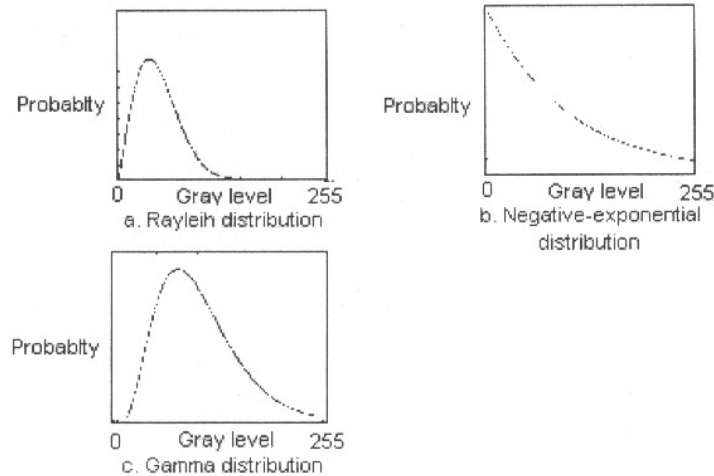
the equation for Gamma noise :

$$P(g)_{Gamma} = \frac{g^{\alpha-1}}{(\alpha - 1)! \alpha^\alpha} \quad (2-17)$$

Where variance $=\alpha^2 \alpha$

The histogram of negative exponential noise is actually gamma noise with the peak moved to the origin ($\alpha= 1$) [6].

Fig (2-4) shows the noise histogram,



Fig(2-4) Image noise histogram[6].

There are two types of noise: [3]

- a. Additive noise,
- b. Multiplicative noise.

a. Additive Noise

Noise is linear additive to image that is independent of the strength input signal. The probability density function is represented by the Gaussian distribution with mean equal to zero. The noise, also, assumed white because the spectrum of it is approximately constant. This situation is similar when a picture is scanned by television camera. The mathematical representation as eq. (2-7), where $n(x,y)$ is additive noise [3].

b. Multiplicative Noise:

This type of noise depending on the input signal is multiplicative or correlated with the original signal. This type is representing by Poisson distribution [3].

2.4 Image Restoration

Image restoration methods are used to improve the appearance of an image by application of restoration process that uses a mathematical model for image degradation,

A number of different techniques has been proposed for digital image restoration, some of these techniques are applied in frequency domain others in spatial domain. The aim of these restoration techniques is to make as good an estimate as possible of the original picture or scene $f(x,y)$ [10].

Image restoration techniques may be classified as follows;

- Linear restoration techniques.
- Non linear restoration techniques.

2.4.1 Image Restoration Algorithms

In this section we will assume that the PSF is satisfactorily known. A number of methods will be introduced for removing the blur from the recorded image " $g(x,y)$ " using a linear filter. If the point-spread function of the linear restoration filter, denoted by $h(x,y)$, has been designed, the restored image is given by [23]:

$$g(x, y) = h(x, y) * f(x, y) \quad (2-18)$$

$$= \sum_{k_1=0}^{N-1} \sum_{k_2=0}^{M-1} h(k_1, k_2) f(x - k_1, y - k_2)$$

in the frequency domain eq.(2-19) is given by:

$$G(u, v) = H(u, v)F(u, v)$$

where:

$G(u, v)$ = Fourier transform of the degraded image.

$H(u, v)$ = Fourier transform of the degraded function.

$F(u, v)$ = Fourier transform of the original image.

The objective of this section is to design appropriate restoration filters $H(u,v)$ [23].

a. Frequency Domain Filters

Frequency domain filtering operates by using Fourier domain transform representation of images. This representation consists of information about the spatial frequency content of the image, also referred to as spectrum of the image [6]. Some types of frequency domain filter are:

1. Inverse Filter

The inverse filter uses the degradation model in the frequency domain, with the add assumption of no noise ($N(u,v) = 0$). If this is the case, the Fourier transform of the degraded image is [6]:

$$G(u,v) = H(u,v) \hat{F}(u,v) + N(u,v) \quad (2-19)$$

So the Fourier transform of the original image can be found as follows:

$$\hat{F}(u,v) = \frac{G(u,v)}{H(u,v)} = G(u,v) \frac{1}{H(u,v)} \quad (2-20)$$

Where $\hat{F}(u,v)$ is the Fourier transform of estimated (restored) image. To find the original image, the inverse Fourier transform has been taken:

$$\hat{f}(x,y) = \mathfrak{F}^{-1} \{ \hat{F}(u,v) \} = \mathfrak{F}^{-1} \{ G(u,v) / H(u,v) \} \quad (2-21)$$

where $\mathfrak{F}^{-1} \{ \quad \}$ represents the inverse Fourier transform [6].

In case of the noise existence, the small ratio values yield a reconstruction of an amplified noise. However, for noisy images, the Fourier transform of the inverse filter is given by;

$$\hat{F}(u, v) = G(u, v) / h(u, v) - N(u, v) / H(u, v) \quad (2-22)$$

This expression clearly indicates that If $H(u, v)$ is zero or become very small, the term $N(u, v) / H(u, v)$ could dominate the restoration result $\mathfrak{F}^{-1} \{ \hat{F}(u, v) \}$. In practice $H(u, v)$ drops off rapidly as a function of distance from the origin of the uv plane. The noise term, however, usually falls off at a much slower rate [5]. One method to deal with this problem is to limit the restoration to a specific radius about the origin in the spectrum, called the restoration cutoff frequency. For spectral components beyond the radius, set the gain filter to zero or one ($G(u, v) = 0$ or 1). This is equivalent to an ideal low pass filter [6].

2. Wiener Filter

The wiener filter is also called a minimum mean-square estimator (developed by Norbert Wiener in 1942), alleviated some of the difficulties inherent in inverse filtering by attempting to model the error in the restored image through the use of statistical methods. After the error is modeled, the average error is mathematically minimized, thus the term minimum mean-square estimator. The resulting equation is the Wiener filter [6]:

$$R_w(u, v) = \frac{H^*(u, v)}{|H(u, v)|^2 + \left[\frac{S_n(u, v)}{S_f(u, v)} \right]} \quad (2-23)$$

where $H^*(u, v)$ is the complex conjugate of $H(u, v)$.

$S_n(u, v) = |H(u, v)|^2$ is the power spectrum of the noise.

$S_f(u,v) = \left| \hat{F}(u,v) \right|^2$ is the power spectrum of the original image.

The ratio $S_n(u,v) / S_f(u,v)$ is called the noise to signal ratio is given by [25]:

$$\frac{S_n(u,v)}{S_f(u,v)} = \frac{1}{(SNR)^2} \quad (2-24)$$

where

SNR =signal to noise ratio[25]:

$$R_w(u,v) = \frac{H^*(u,v)}{|H(u,v)|^2 + \left[\frac{1}{(SNR)^2} \right]} \quad (2-25)$$

If the noise term $S_n(u,v)$ is zero for all relevant values of u and v , this ratio becomes zero and the Wiener Filter reduces to the inverse filter [25].

As the noise term increases, the denominator of the Wiener filter increases thus decreases the value of $R_w(u,v)$ [6].

In practical applications, the original uncorrupted image is not typically available, so the power spectrum ratio is replaced by the parameter K whose optimal value must be experimental determined [6]; i.e:

$$R_w(u,v) = \frac{H^*(u,v)}{|H(u,v)|^2 + K} \quad (2-26)$$

Making the K parameter a function of the frequency domain variables (u,v) may also add some benefits. Because the noise typical dominates at high frequency, it seems to have the value of K increase as

the frequency increases, which will case the filter to attenuate the signal at high frequency [6].

In the Fourier transform of the restored image " $\hat{F}(u, v)$ " using Wiener filter, is given by [6]:

$$\hat{F}(u, v) = R_w(u, v) * G(u, v) \quad (2-27)$$

The final restoration result is obtained by the inverse FT of the above equation, i.e [25]:

$$\hat{f}(x, y) = \mathcal{F}^{-1} \left\{ \left| \hat{F}(u, v) \right|^2 \right\} \quad (2-28)$$

3. Constrained Least-Squares Filter

The constraint least-squares filter provides a filter that can eliminate some of the artifacts caused by other frequency filters. This is done by including a smoothing criterion in the filter derivation, so that the result will not have undesirable oscillations (these appear as "waves" in the image), as sometimes occur with other frequency domain filters. The constrained least-square filter is given by [6]:

$$R_{CLS}(u, v) = \frac{H^*(u, v)}{|H(u, v)|^2 + \gamma[p(u, v)]^2} \quad (2-29)$$

where γ =adjustment factor .

$p(u, v)$: the Fourier transform of the smoothness criterion.

If γ is zero we have an inverse filter solution [25].

The adjustment's factor value is experimentally determined and is application dependent. A standard function to use for $p(x, y)$ (the inverse Fourier transform of $P(u, v)$) is the laplacian filter mask, as follows [6]:

$$p(x, y) = \begin{vmatrix} 0 & -1 & 0 \\ -1 & 4 & -1 \\ 0 & -1 & 0 \end{vmatrix} \quad (2-30)$$

b. Iterative image restoration algorithms

There are many forms of iterative restoration algorithms, from the basic iterative algorithms to the regularized constrained ones. Biemond and Katsaggelos provided an excellent tutorial of iterative image restoration algorithms respectively [26].

Iterative techniques are used in this work for restoring noisy-blurred images. Among the advantages of iterative approaches are the following:

- (i) there is no need to determine or to implement the inverse of an operator;
- (ii) knowledge about the solution can be incorporated into the restoration process;
- (iii) the solution process can be monitored as it progresses;
- (iv) constraints can be used to control the effect of noise;
- (v) parameters determining the solution can be updated as the iteration progresses.

Tikhnov and Arsenin were the first to study exclusively the concepts of regularization, although some important prior work had been performed by Phillips, Twomey, and number of Russian mathematicians[27].

Although originally formulated for the space - invariant case, it can be applied to the spatially varying case as well. Neglecting, for a moment, the noise contribution and making use of the compact matrix – vector notation introduced in (2-4) to denote both the space – varying and space – invariant cases, the following identity is introduced, which must hold for all values of the parameter β [27] :

$$f^{k+1} = f^k + \beta(g - Hf^k) \quad (2-31)$$

Applying the method of successive substations to this suggest the following iteration [27].

The base scheme of iterative image restoration is the method of successive approximation which is often applied to the solution of linear algebraic system of equations [28]:

$$\hat{f}^{k+1} = \hat{f}^k + \beta H^T (g - H\hat{f}^k) \quad (2-32)$$

$$\hat{f}^0 = \beta H^T g \quad (2-33)$$

Where \hat{f}^{k+1} is the estimation of f on $k+1$ iteration, β is a relaxation parameter, “^T” denotes matrix transpose. The relaxation parameter controls The convergence of iterations and is determined as [28]

$$0 < \beta \leq 2\|H^T H\|^{-1} \quad (2-34)$$

The solution obtained after infinite number of iterations converges to the result of inverse filtering. To constrain the influence of noise the finite number of iterations was usually chosen that was the first way of regularization in iterative methods [29]:

Tikhnov (Tikhnov and Arsenin.1977) introduced the following functional that has be minimized to obtain a stable estimation for f [29]:

$$\phi(f) = \frac{1}{2} (\|Hf - g\|^2 + \alpha \|Cf\|^2) \quad (2-35)$$

Where $\|\cdot\|^2$ is the Euclidean norm. the regularization parameter determinates a tradeoff between the fitting represented by the $\|Hf - g\|^2$ term and the smoothing that is introduced by the term $\|Cf\|^2$ [29].

If no additional constraints are imposed this problem is linear and the solution is given by [29]:

$$\hat{f} = \frac{H^T g}{H^T H + \alpha C^T C} \quad (2-36)$$

The introduction of the general regularization theory into iterative process allowed to essentially increase the algorithm noise immunity. The generalized scheme of iterative method with Tikhonov regularization could be written as [28]:

$$\begin{aligned}\hat{f}^{k+1} &= (I - \alpha\beta C^T C)\hat{f}^k + \beta H^T (g - H\hat{f}^k) \\ &= (I - \beta(H^T H + \alpha C^T C))\hat{f}^k + \beta H^T Hg\end{aligned}\quad (2-37)$$

Where α is a regularization parameter, C represents high-pass filter obtained from Tikhonov stabilization functional, I is unit matrix [28].

The regularization parameter controls the tradeoff between fidelity to the data and smoothness of the solution, and therefore its determination is very important issue [30].

The operator C was chosen as the Laplasian operator given as the mask [28]:

$$\begin{bmatrix} 0 & -1 & 0 \\ -1 & 4 & -1 \\ 0 & -1 & 0 \end{bmatrix}\quad (2-38)$$

The regularized solution after k iterations is given in terms of the eigenvalues and eigenvectors of the blurring[28].

The corresponded condition for relaxation parameter β is given by [28]:

$$0 < \beta \leq 2\|H^T H + \alpha C^T C\|^{-1}\quad (2-39)$$

Katsaggelos *et al.* recognize that the term $(I - \alpha\beta C^T C)$ behaves like a low – pass filter, suppressing the noise amplification in the iterates. As the characteristics of this stabilizing term are obviously related to the properties of the original image, they proposed to compress this term into one single low pass operator C_s , which would reflect spectral knowledge about the original image[28].

where $C_s = I - \alpha\beta C^T C$. It was proposed to change it on Wiener filter for optimal filtering[28].

$$\begin{aligned}\hat{f}^{k+1} &= C_s \hat{f}^k + \beta H^T (g - H\hat{f}^k) \\ &= (C_s - \beta H^T H) \hat{f}^k + \beta H^T Hg\end{aligned}\quad (2-40)$$

The propose to consider the regularization as a generalized smoothing of the image that could be accomplished by any known method of noise removal.

One choice for C_s is the noise smoothing wiener filter, which assume the form[28]:

$$C_s = S_{ff} (S_{ff} + S_{mn})^{-1} \quad (2-41)$$

where S_{ff} and S_{mn} are covariance matrices (autocorrelation matrices)[27], of the initial image and noise, which supposed to be known *a priori*. If these matrices were known a priori, it would be possible to use this information not only for image smoothing, but also for phase retrieval that could lead to better results [27].

The advantage of eq. (2-40) over eq. (2-37) is that the interpretation of (2-40) is more clear. In practice construction of a suitable filter, C_s is sometimes earlier than the selection of regularizing operator C [27].

Another methods for incorporating deterministic constrains into the restoration process is to extend the basic iterations which is given [27]:

$$\hat{f}^{k+1} = P[(I - \alpha\beta C^T C) \hat{f}^k + \beta H^T (g - H\hat{f}^k)] \quad (2-42)$$

Where P is again a projection onto a convex set C .

The equation (2-42) is usually small, the number of constraints ,and the convergence speed[27].

3.5 Image Quality

In image processing systems, certain amount of errors in the restored image is tolerated. In this case fidelity criterion can be used as a measure of system quality. Objective measures or quantitative tests of image quality can be classified into two classes; these are uni-variant and bi-variant measures. The uni-variant measure is a numerical rating assigned to a single image, while the bi-variant measure is a numerical comparison between pair of images. Since in our research, the problem is to measure the fidelity of a restoration method where a pair of images can, always, be provided (i.e. original and restored images), thus we shall turn our concern to describe some of the bi-variant measures [8].

The quality required naturally depends on the purpose for which an image is used [3].

Methods for assessing image quality can be divided into two categories [3]:

1- Objective

2- Subjective

The objective fidelity criteria are borrowed from digital signal processing and information theory and provide us with equations that can be used to measure the amount of error in the reconstructed image.

Commonly used objective measures are Root Mean Squares Error "MSE" signal-to-noise ratio SNR_{RMS} , and the peak signal-to-noise ratio (SNR_{peak}) [6].

If we assume that $f(x, y)$ =the original image

$\hat{f}(x, y)$ =the reconstructed image.

The error between an input image $f(x,y)$ and corresponding restored image $\hat{f}(x,y)$ is given by[8]:

$$e(x,y) = f(x,y) - \hat{f}(x,y) \quad (2-43)$$

The squared error averaged over the image array is then

$$MSE = \frac{1}{MN} \sum_{x=0}^{N-1} \sum_{y=0}^{M-1} e^2(x,y) \quad (2-44)$$

$$MSE = \frac{1}{MN} \sum_{x=0}^{N-1} \sum_{y=0}^{M-1} [f(x,y) - \hat{f}(x,y)]^2 \quad (2-45)$$

The root-mean-square error is found by taking the square root of the error squared divided by the total number of pixels in the image [5]:

$$RMSE = \sqrt{\frac{1}{N^2} \sum_{x=0}^{N-1} \sum_{y=0}^{N-1} [\hat{f}(x,y) - f(x,y)]^2} \quad (2-46)$$

The smaller the value of the error metrics, the better the reconstructed image represents the original image.

Alternately, with the signal to noise value, a large number imply a better image. The (SNR) value consider the reconstructed image $\hat{f}(u,v)$

To be the "signal" and error to be the "noise" .We can define the mean –square signal to noise ratio as[3]:

$$SNR_{RMS} = \sqrt{\frac{\sum_{x=0}^{N-1} \sum_{y=0}^{N-1} [\hat{f}(x,y)]^2}{\sum_{x=0}^{N-1} \sum_{y=0}^{N-1} [\hat{f}(x,y) - f(x,y)]^2}} \quad (2-47)$$

Another related value, the peak signal-to noise ratio, is define as:

$$SNR_{peak} = 10 \log_{10} \frac{(L-1)^2}{\frac{1}{N^2} \sum_{x=0}^{N-1} \sum_{y=0}^{N-1} [\hat{f}(x,y) - f(x,y)]^2} \quad (2-48)$$

Where L the number of grey levels

(e.g. for 8 bits L=256).

It is important to define the ratio of signal to noise in a way which is consistent with the nature of optical images. The signal to noise ratio "SNR" can be defined as the ratio of signal variance (σ_f^2) to that of the noise variance (σ_n^2) [3]:

$$SNR = \frac{\sigma_f^2}{\sigma_n^2} \quad (2-49)$$

where

$$\sigma_f^2 = \langle \{f - \langle f \rangle\}^2 \rangle$$

$$\sigma_n^2 = \langle \{n - \langle n \rangle\}^2 \rangle$$

$\langle \rangle$ is the mean.

f = the original signal

n = the noise signal.

Since $\langle n \rangle = 0$, therefore $\sigma_n^2 = \langle n^2 \rangle$

Subjective fidelity criteria require the definition of a qualitative scale to assess image criteria. The results are then analyzed statistically, typically using the averages and standard deviations as metrics. Subjective fidelity measures can be classified into three categories:

- 1- They are referred to as impairment tests, where the test subjects in terms of how bad they are.

- 2- The quality tests, where the test subjects rate the images in terms of how good they are.
- 3- The comparison tests, where the image are evaluated on a side-by-side basis.

The subjective measure are better method for comparison of reconstructed algorithms, if the goal is to achieve high quality images as defined by our visual perception [6].

For this reason, normalize Cross Correlation Coefficient "CCC" is given by [3] :

$$CCC = \frac{\langle (f(x,y)\hat{f}(x,y) - \langle f(x,y) \rangle \langle \hat{f}(x,y) \rangle) \rangle}{\left[\langle (f(x,y) - \langle f(x,y) \rangle)^2 \rangle \langle (\hat{f}(x,y) - \langle \hat{f}(x,y) \rangle)^2 \rangle \right]^{1/2}} \quad (2-50)$$

where $f(x,y)$ = is the standard or ideal image .


$\hat{f}(x,y)$ = is an approximation of the standard field.

The range of CCC is between (-1 to 1). If $CCC = 1$, the imply perfect correlation (i.e. $\hat{f}(x,y) = f(x,y)$), $(1-c)$ is measure of the error. The SNR in terms of C is imply given by [3]:

$$SNR = \left(\frac{CCC}{1-CCC} \right)^{1/2} \quad (2-51)$$



CHAPTER THREE



RESULTS
and
DISCUSSION

3.1 Introduction

There are many sources of blur. The focusing atmospheric turbulence blur which arises, e.g., in remote sensing and astronomical imaging due to short and long-term exposures through the atmosphere. The turbulence in the atmosphere gives rise to random variations in the refractive index. For many practical purposes, and for long exposure, this blurring can be modeled by a Gaussian point spread function [31].

The purpose of image restoration is to "compensate for" or "undo" defects which degrade an image. Degradation comes in many forms such as motions blur noise. In cases like motion blur, it is possible to come up with a very good estimate of the actual blurring function and "undo" the blur to restore the original image. In this research, introduce and implement several of the methods are used in the image processing world to restore images.

Linear methods of image restoration are usually capable of being *computed* in a straight forward and economical [32].

Nonlinear methods of image restoration are usually requiring much more elaborate and closely computational procedures [32].

The Matlab language has been used to restoration image for satellite image with image size 256 x 256 pixels. The different types of restoration filters are adapted, these are, Inverse filter, Least-Squares Filter (Wiener filter), Constrained Least-Squares Filter (Regular Filter), and Iterative restoration (Tikhonov filter).

3.2 Practical Part

In this chapter, the different types of restoration filters can be adopted, these are:

1. Inverse filter
2. Least-Squares Filter (Wiener filter)
3. Constrained Least-Squares Filter (Regular Filter)
4. Iterative restoration (Tikhonov filter)

Also, Gaussian PSF were adopted with different standards deviation values " σ ", $\sigma = 0.5, 1, \text{ and } 2$.

Also, have been used two different type of noise these are:

1. Gaussian noise, with different noise level i.e. different SNR, SNR=5, 10, and 20, with zero mean.
2. Salt and pepper noise, with different noise density " d ", $d = 0.05, \text{ and } 0.1$.

Moreover, we have been used different regularization parameter " α " $\alpha = 0, \text{ and } 0.5$.

All restoration techniques are used with image size 256×256 pixels.

Image Restoration Algorithm

- 1- Read color image of size 256×256 type RGB.
- 2- Simulate degraded image (blurred and noisy) with different standards deviation " σ ", and with different noise level.
- 3- RGB degraded image has been separated to their component, i.e. Red, Green, and Blue components.
- 4- Restoration filters are applied to each component of image, (using inverse filter, Least-Squares Filter (Wiener filter), constrained Least-Squares Filter (Regular Filter), and iterative restoration (Tikhonov filter) then returned to RGB image format.
- 5- Calculate the mean square error (MSE) for each component of restored RGB image.

Figure (3-1): shows flowchart of the program

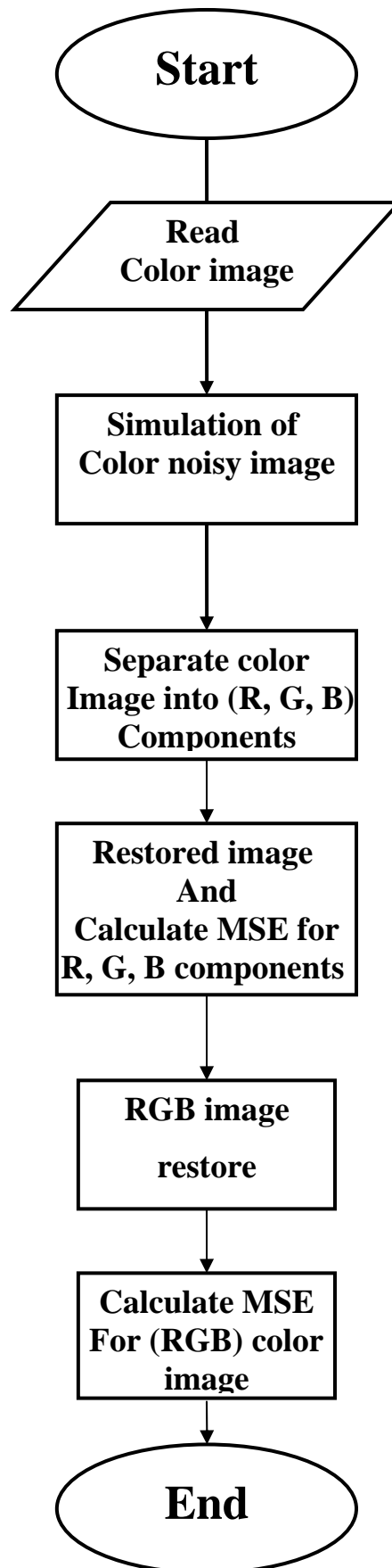


Figure (3-1) Flowchart of Image Restoration Algorithm

3.3 Results

A color Jpeg image of 256×256 pixels size , "satellite image", as shown in Figure(3-2),was used to check the quality of the restoration techniques.



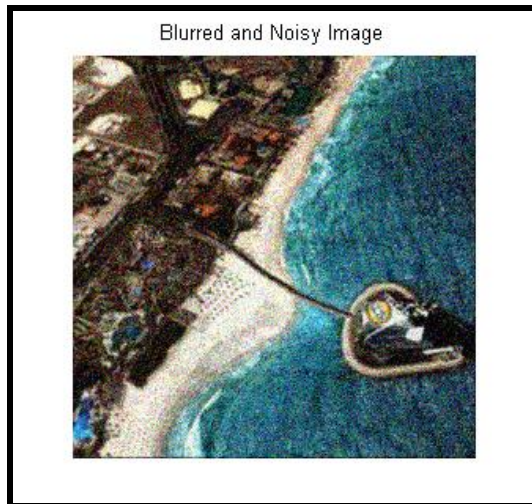
Figure(3-2) Original satellite image [33].

The degraded (blurred and noisy) images are simulated as follows:

1. The blurred images were simulated by convolving the original image with Gaussian function of different standard deviation " σ ", $\sigma = 0.5, 1, \text{ and } 2$.
2. Random noise of Gaussian distribution with zero means was added to the blurred image. Different SNR = 5, 10, and 20, Also, noise of salt and pepper distribution with noise density " d ", $d = 0.05, \text{ and } 0.1$) was added to the blurred image.

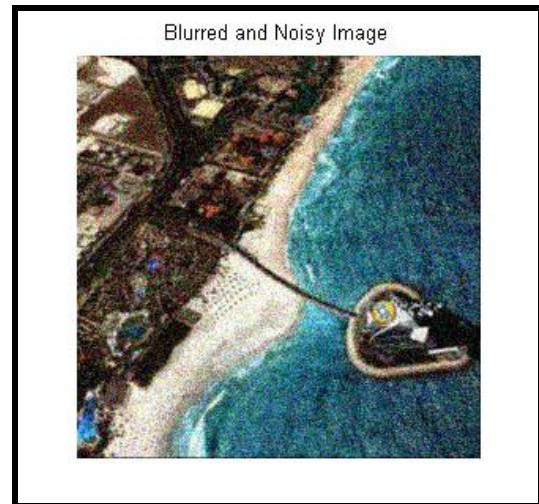
Figure (3-3) shows the degraded image with Gaussian blur and Gaussian noise with different parameter of degradation , where

a : represent degraded image with $\sigma = 0.5$, and SNR =5, b : represent degraded image with $\sigma = 0.5$, and SNR =10, and c : represent degraded image with $\sigma = 0.5$, and SNR =20. The figure shows, also, the Mean Square Error (MSE) of the degraded image with respect to the original image.



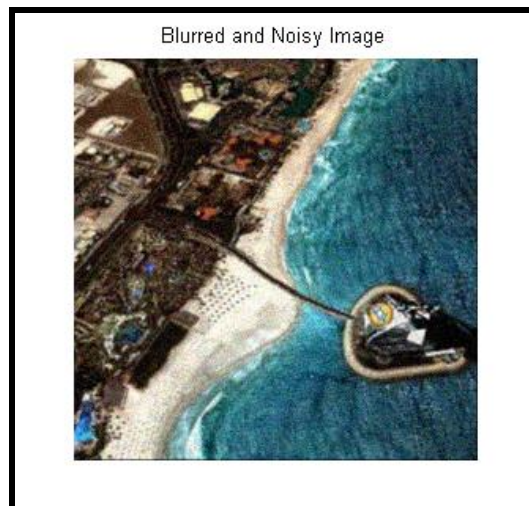
(a)

MSE = 14.5667



(b)

MSE = 10.4162

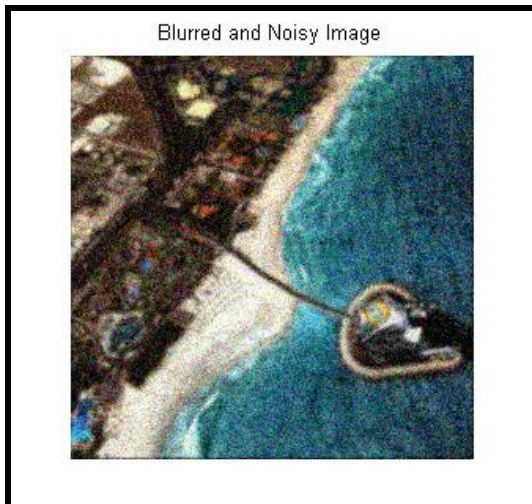


MSE = 8.2159

Figure(3-3) degraded image
with $\sigma = 0.5$, and SNR =5,10,20 respectively

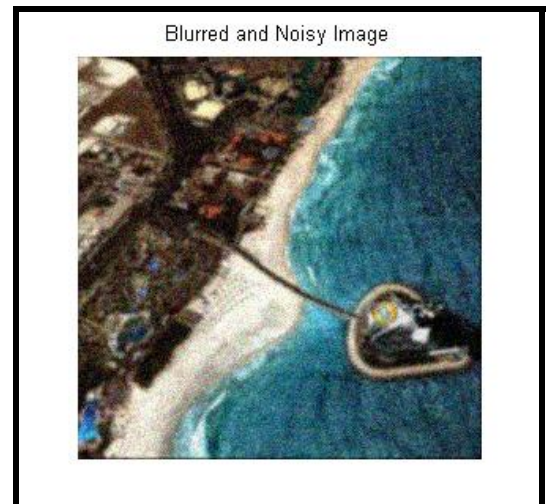
Figure (3-4) shows the degraded image with Gaussian blur and Gaussian noise with different parameter of degradation, where

a : represent degraded image with $\sigma = 1$, and SNR =5, b : represent degraded image with $\sigma = 1$, and SNR =10, and c : represent degraded image with $\sigma = 1$, and SNR =20. The figure shows, also, the Mean Square Error (MSE) of the degraded image with respect to the original image.



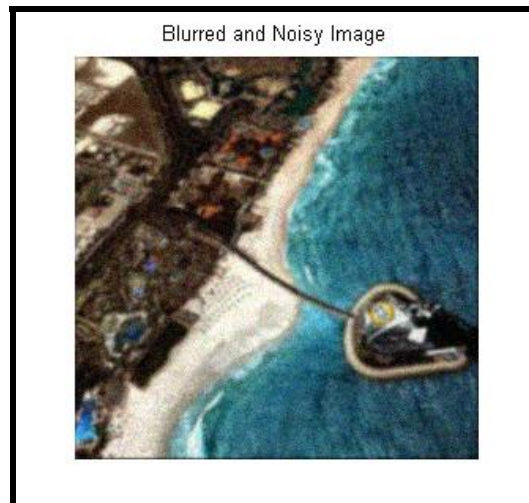
(a)

MSE = 15.0624



(b)

MSE = 11.059



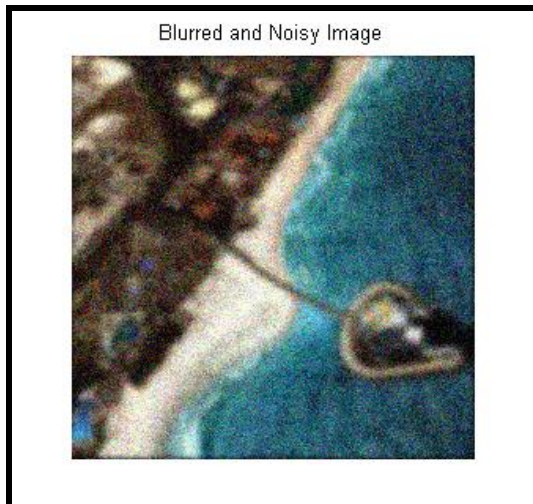
(c)

MSE = 8.9195

Figure(3-4) degraded image
with $\sigma = 1$, and SNR =5,10,20 respectively

Figure (3-5) shows the degraded image with Gaussian blur and Gaussian noise with different parameter of degradation, where

a : represent degraded image with $\sigma = 2$, and SNR =5, b : represent degraded image with $\sigma = 2$, and SNR =10, and c : represent degraded image with $\sigma = 2$, and SNR =20. The figure shows, also, the Mean Square Error (MSE) of the degraded image with respect to the original image.



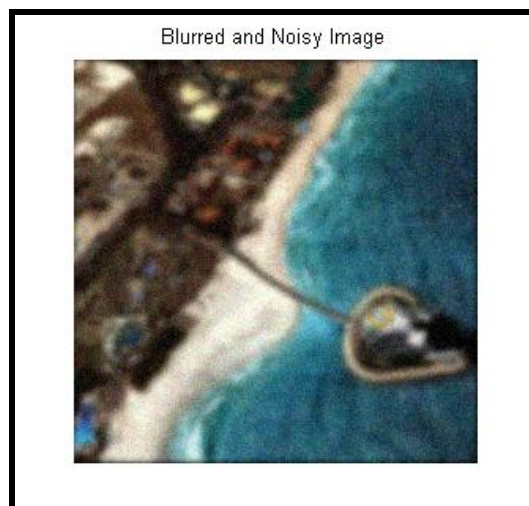
(a)

MSE = 17.4375



(b)

MSE = 13.6742



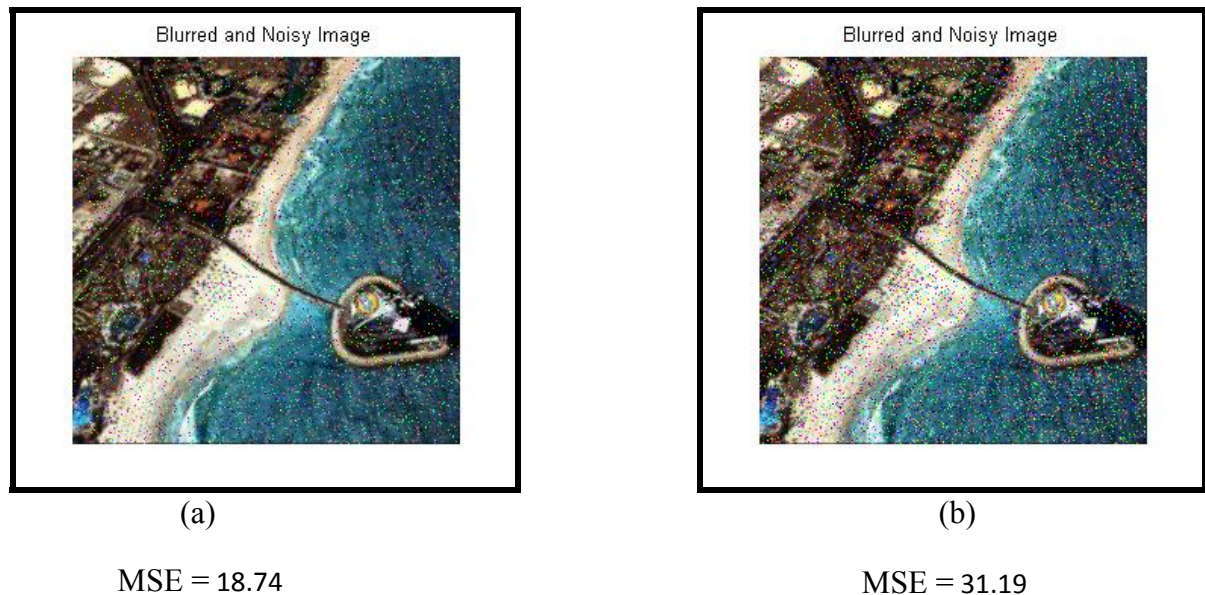
(c)

MSE = 11.8203

Figure(3-5) degraded image
with $\sigma = 1$, and SNR =5,10,20 respectively

Figure (3-6) shows the degraded image with Gaussian blur and with Salt and Pepper noise with different parameter, where

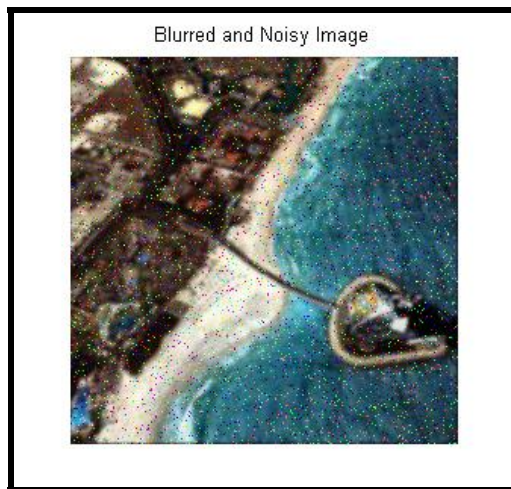
a : represent degraded image with $\sigma = 0.5$, and $d = 0.05$, b : represent degraded image with $\sigma = 0.5$, and $d = 0.1$. The figure shows, also, the Mean Square Error (MSE) of the degraded image with respect to the original image.



Figure(3-6) degraded image with $\sigma = 0.5$, and Noise density =0.05,0.1 respectively

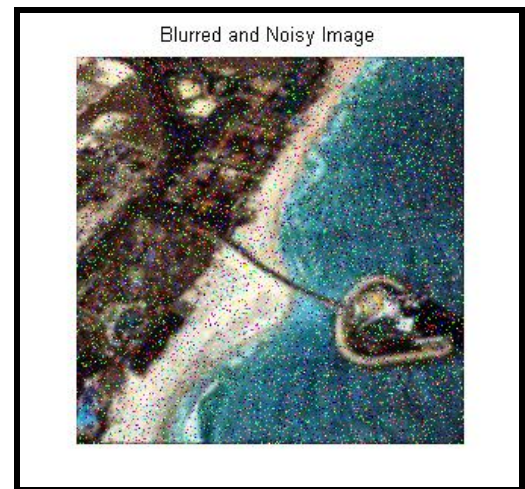
Figure (3-7) shows the degraded image Gaussian blur, and with Salt and Pepper noise with different parameter of degradation, where

a : represent degraded image with $\sigma = 1$, and $d = 0.05$, b : represent degraded image with $\sigma = 1$, and $d = 0.1$. The figure shows, also, the Mean Square Error (MSE) of the degraded image with respect to the original image.



(c)

MSE = 19.44



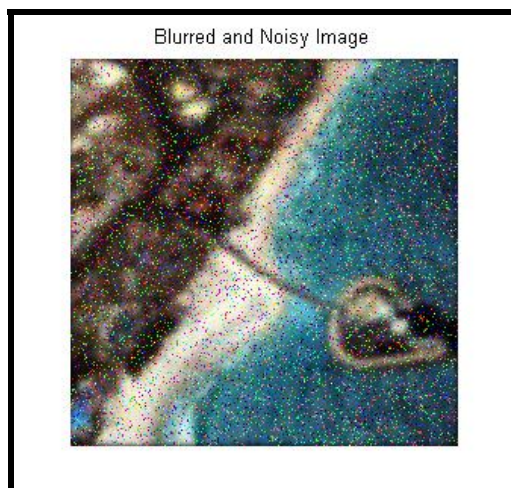
(d)

MSE = 32.26

Figure(3-7) degraded image
with $\sigma = 1$, and Noise density =0.05,0.1 respectively

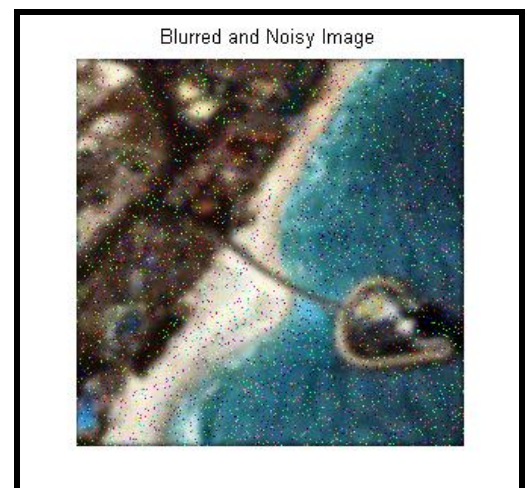
Figure (3-8) shows the degraded image Gaussian blur and with Salt and Pepper noise with different parameter of degradation , where

a : represent degraded image with $\sigma = 2$, and d =0.05, b : represent degraded image with $\sigma = 2$, and d =0.1. The figure shows, also, the Mean Square Error (MSE) of the degraded image with respect to the original image.



(a)

MSE = 22.394

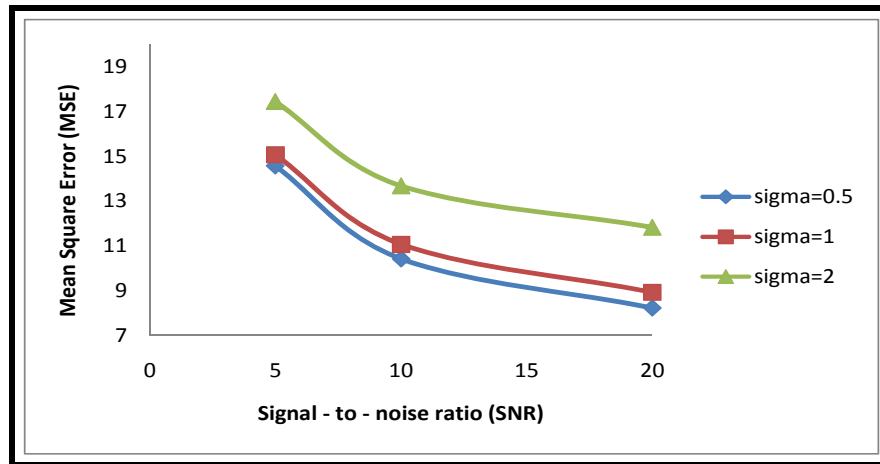


(b)

MSE = 34.97

Figure(3-8) degraded image
with $\sigma = 2$, and Noise density =0.05,0.1 respectively

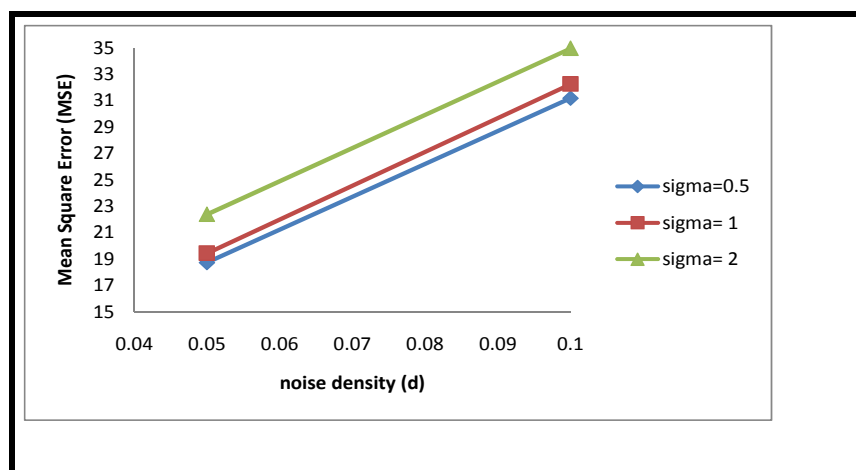
Figure (3-9) represent Mean Square Error (MSE) Versus Signal to Noise Ratio "SNR" , using Gaussian noise for different with SNR= 5,10, and 20 , and using different sigma " σ ", $\sigma = 0.5, 1, \text{ and } 2$ for Gaussian blur.



Figure(3-9)

Mean Square Error (MSE) Versus Signal to Noise Ratio "SNR".

Figure (3-10) represent Mean Square Error (MSE) Versus Noise Density (d), using Salt and Pepper noise for different noise density "d", $d=0.05, \text{ and } 0.1$ and using different with of standard deviation " σ ", $\sigma = 0.5, 1, \text{ and } 2$ for Gaussian blur.



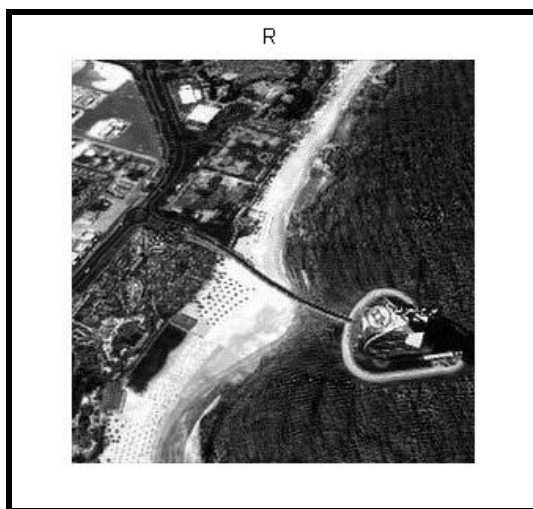
Figure(3-10)

Mean Square Error (MSE) Versus Noise Density (d).

1. Inverse Filter

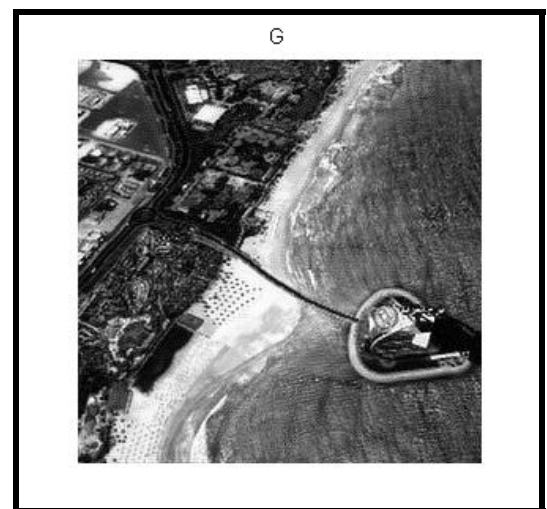
Figure (3-11) represent the restored image of the degraded image with Gaussian Point Spread Function and Gaussian noise, with $\sigma = 0.5$, and SNR=5.

a : represent the restored image for red component, b: represent the restored image for green component, c: represent the restored image for blue component, and d: represent the restored image for RGB image , using inverse filter. The figure shows, also, the (MSE) of the degraded image with respect to the original image.



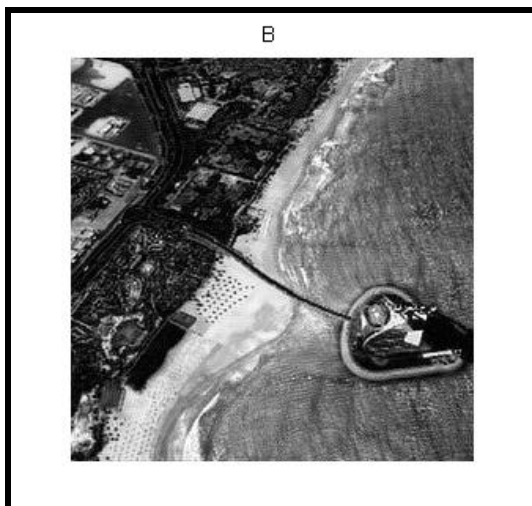
(a)

MSE = 0.6154



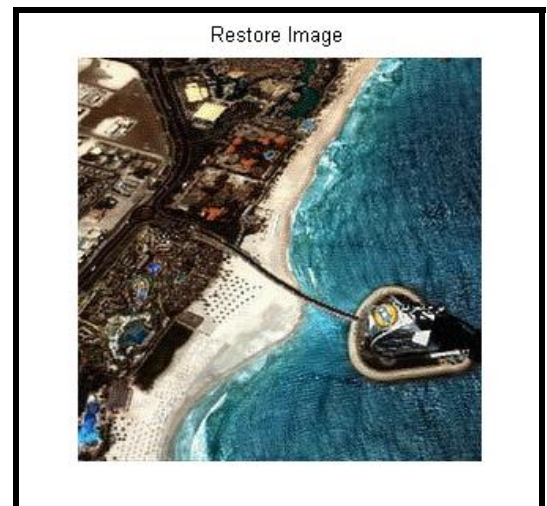
(b)

MSE = 0.6141



(c)

MSE = 0.6040

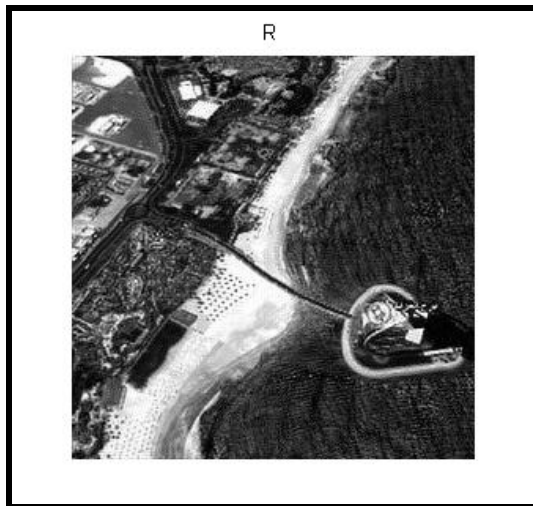


(d)

MSE = 1.8335

Figure(3-11) Restored Image for red, green , blue components of image and RGB image respectively .

Figure (3-12) represent the restored image of the degraded image with Gaussian Point Spread Function and Gaussian noise, with $\sigma = 0.5$, and SNR=20. a : represent the restored image for red component, b: represent the restored image for green component, c: represent the restore image for blue component, and d: represent the restored image for RGB image , using inverse filter. The figure shows, also, the (MSE) of the degraded image with respect to the original image.



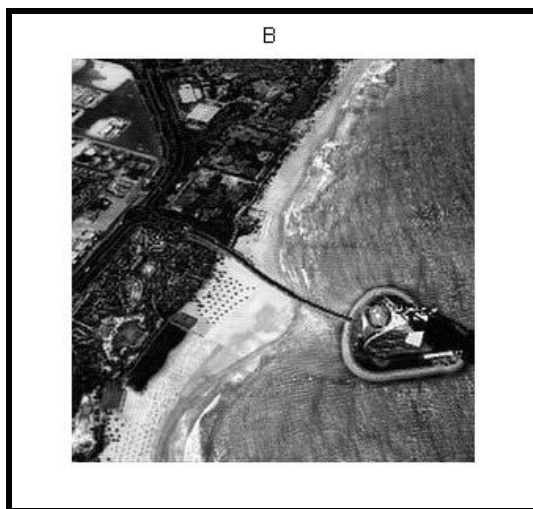
(a)

MSE = 0.6154



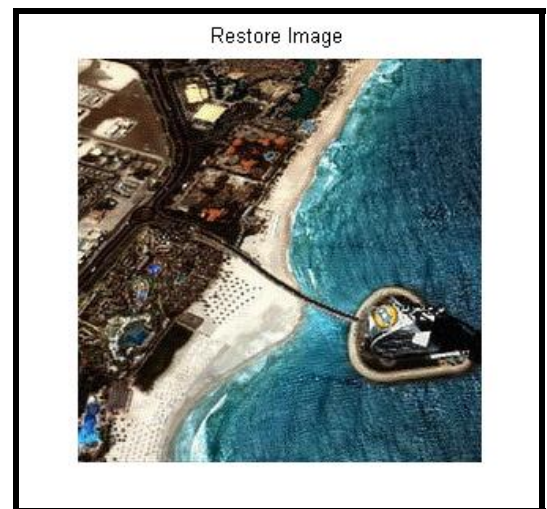
(b)

MSE = 0.6141



(c)

MSE = 0.6040



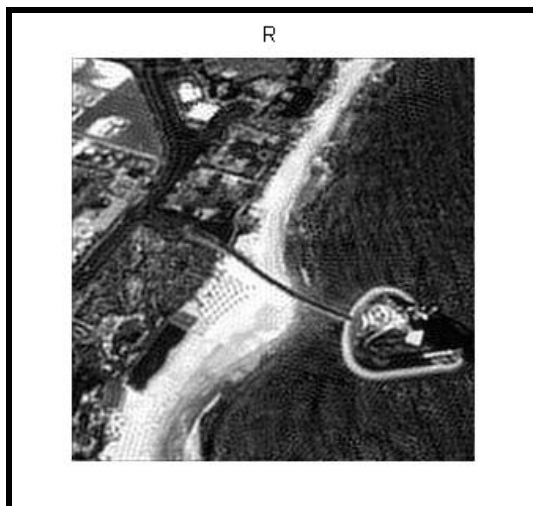
(d)

MSE = 1.8335

Figure(3-12) Restored Image
for red, green , blue components of image and RGB image respectively.

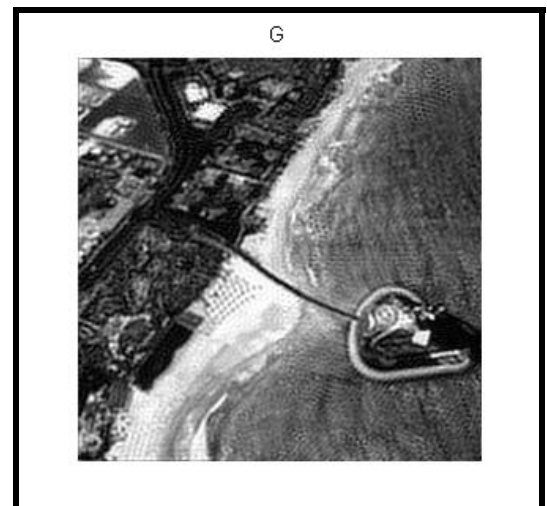
Figure (3-13) represent the restored image of the degraded image with Gaussian Point Spread Function and Gaussian noise, with $\sigma = 1$, and SNR=5.

a : represent the restored image for red component, b: represent the restored image for green component, c: represent the restored image for blue component, and d: represent the restored image for RGB image , using inverse filter. The figure shows, also, the (MSE) of the degraded image with respect to the original image.



(a)

MSE = 1.6103



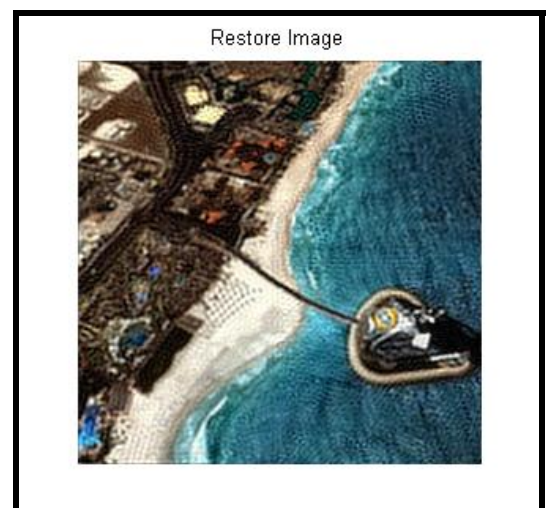
(b)

MSE = 1.6031



(c)

MSE = 1.5783



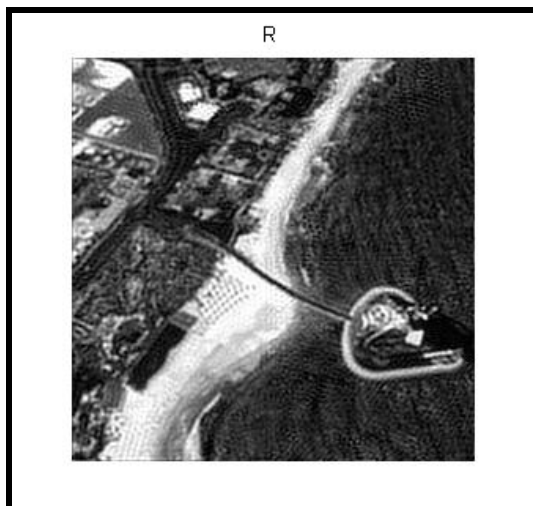
(d)

MSE = 4.7918

Figure(3-13) Restored Image for red, green ,blue components of image and RGB image respectively .

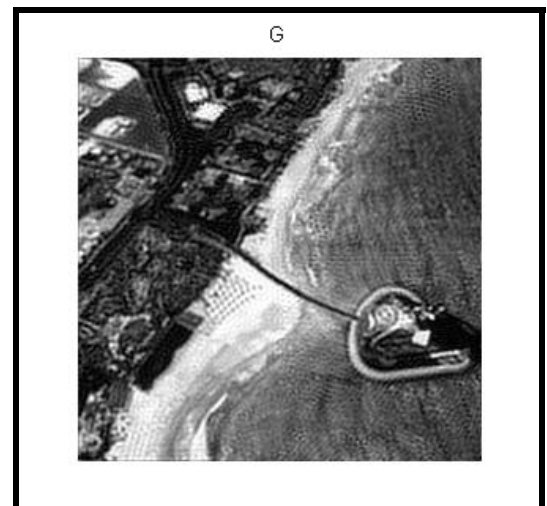
Figure (3-14) represent the restored image of the degraded image with Gaussian Point Spread Function and Gaussian noise, with $\sigma = 1$, and SNR=20.

a : represent the restored image for red component, b: represent the restored image for green component, c: represent the restored image for blue component, and d: represent the restored image for RGB image, using inverse filter. The figure shows, also, the (MSE) of the degraded image with respect to the original image.



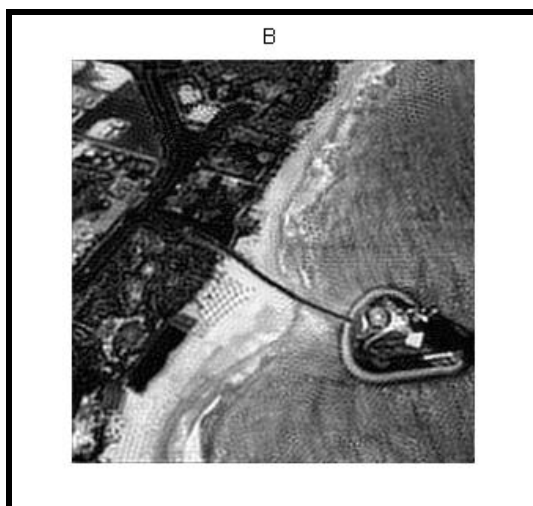
(a)

MSE = 1.6103



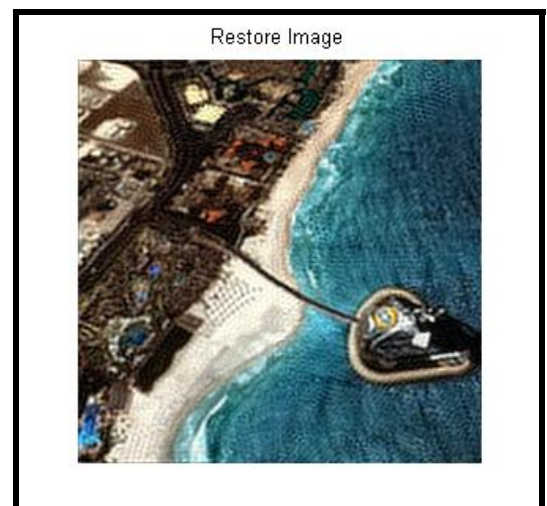
(b)

MSE =1.6031



(c)

MSE =1.5783



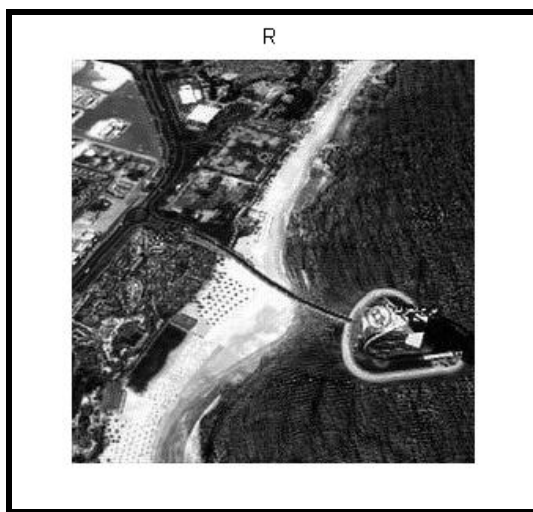
(d)

MSE =4.7918

Figure(3-14) Restored Image for red, green, blue components of image and RGB image respectively.

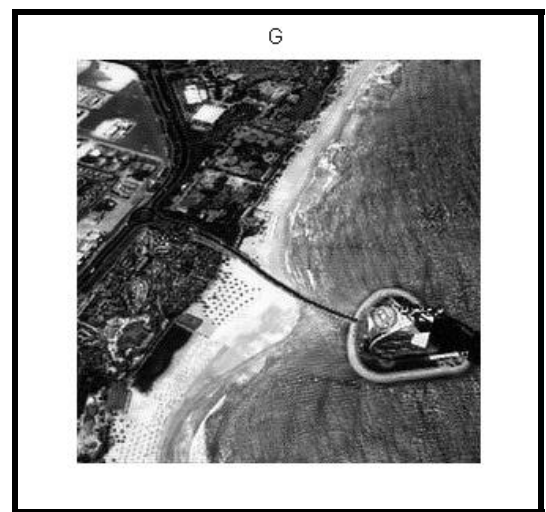
Figure (3-15) represent the restored image of the degraded image with Gaussian Point Speared Function and Salt and Pepper noise, with $\sigma = 0.5$,and $d=0.05$.

a : represent the restored image for red component, b: represent the restored image for green component, c: represent the restored image for blue component, and d: represent the restored image for RGB image , using inverse filter. The figure shows, also, the (MSE) of the degraded image with respect to the original image.



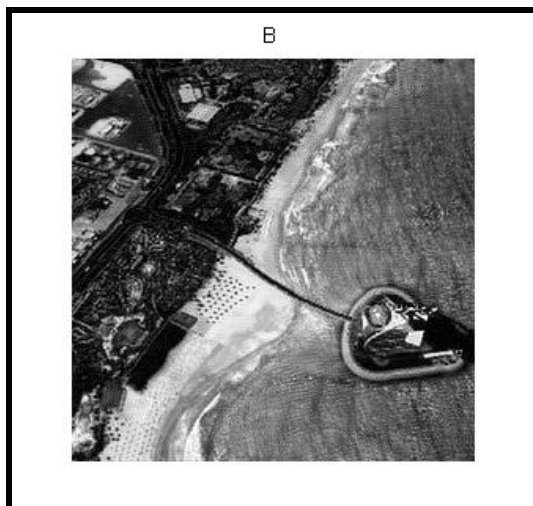
(a)

MSE = 0.6154



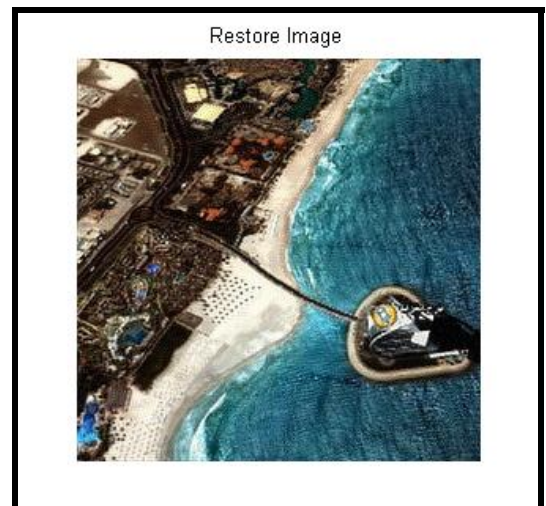
(b)

MSE = 0.6141



(c)

MSE = 0.6040



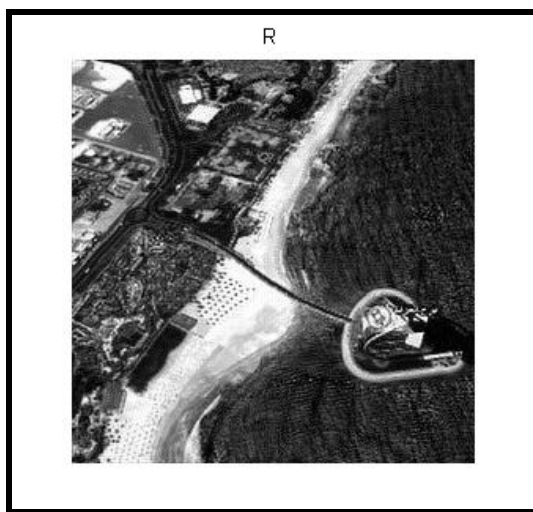
(d)

MSE = 1.8335

Figure(3-15) Restored Image for red, green , blue components of image and RGB image respectively.

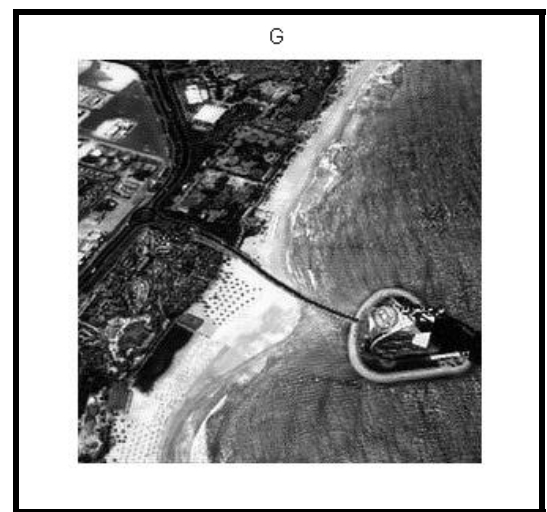
Figure (3-16) represent the restored image of the degraded image with Gaussian Point Speared Function and Salt and Pepper noise, with $\sigma = 0.5$,and $d=0.1$.

a : represent the restored image for red component, b: represent the restored image for green component, c: represent the restored image for blue component, and d: represent the restored image for RGB image , using inverse filter. The figure shows, also, the (MSE) of the degraded image with respect to the original image.



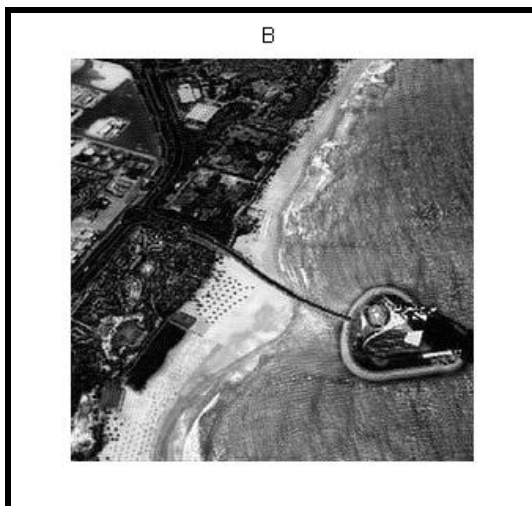
(a)

MSE =0.6154



(b)

MSE = 0.6141



(c)

MSE =0.6040



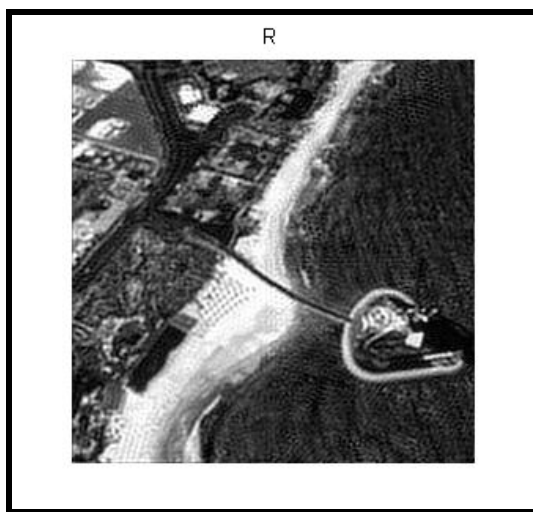
(d)

MSE = 1.8335

Figure(3-16) Restored Image for red, green , blue components of image and RGB image respectively.

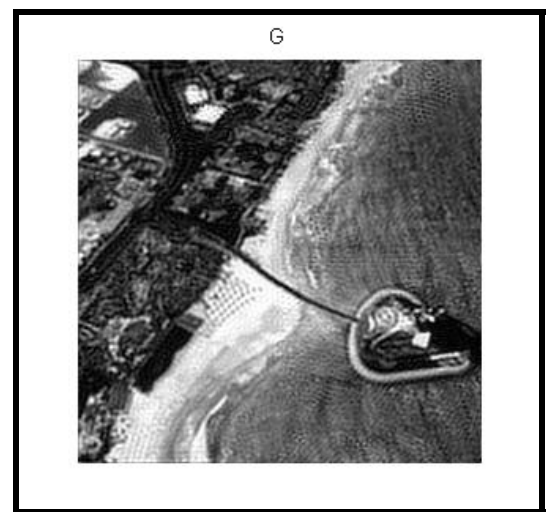
Figure (3-17) represent the restored image of the degraded image with Gaussian Point Speared Function and Salt and Pepper noise, with $\sigma = 1$, and $d=0.05$.

a : represent the restored image for red component, b: represent the restored image for green component, c: represent the restored image for blue component, and d: represent the restored image for RGB image , using inverse filter. The figure shows, also, the (MSE) of the degraded image with respect to the original image.



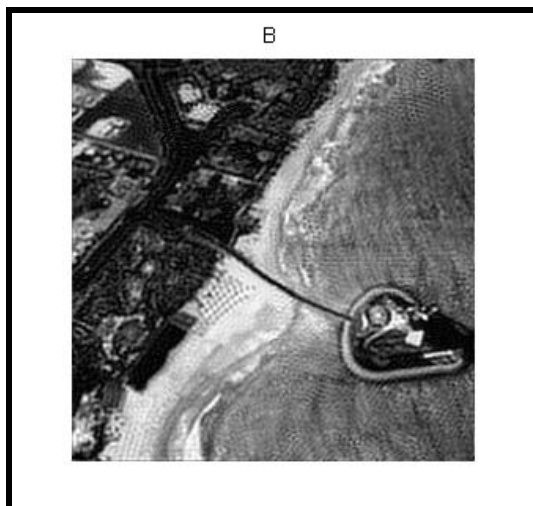
(a)

MSE =1.6103



(b)

MSE =1.6031



(c)

MSE =1.5783

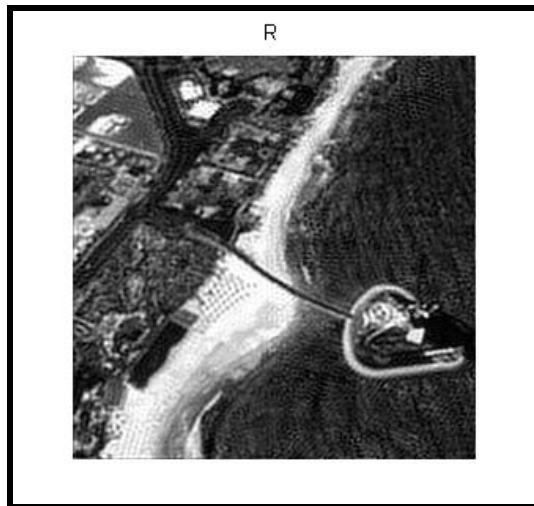


(d)

MSE =4.7918

Figure(3-17) Restored Image
for red, green , blue components of image and RGB image respectively.

Figure (3-18) represent the restored image of the degraded image with Gaussian Point Spread Function and Salt and Pepper noise, with $\sigma = 1$, and $d=0.1$. a : represent the restored image for red component, b: represent the restored image for green component, c: represent the restored image for blue component, and d: represent the restored image for RGB image , using inverse filter. The figure shows, also, the (MSE) of the degraded image with respect to the original image.



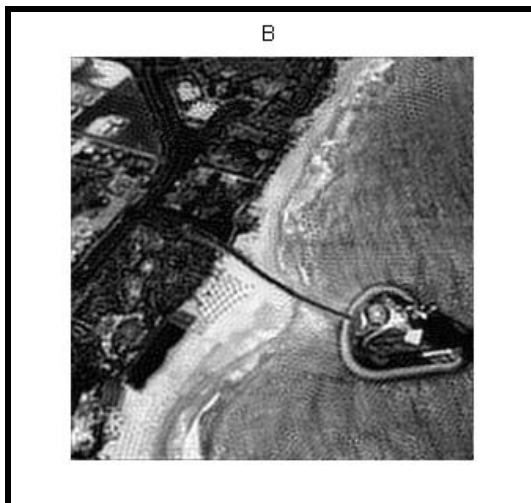
(a)

MSE =1.6103



(b)

MSE =1.6031



(c)

MSE =1.5783



(d)

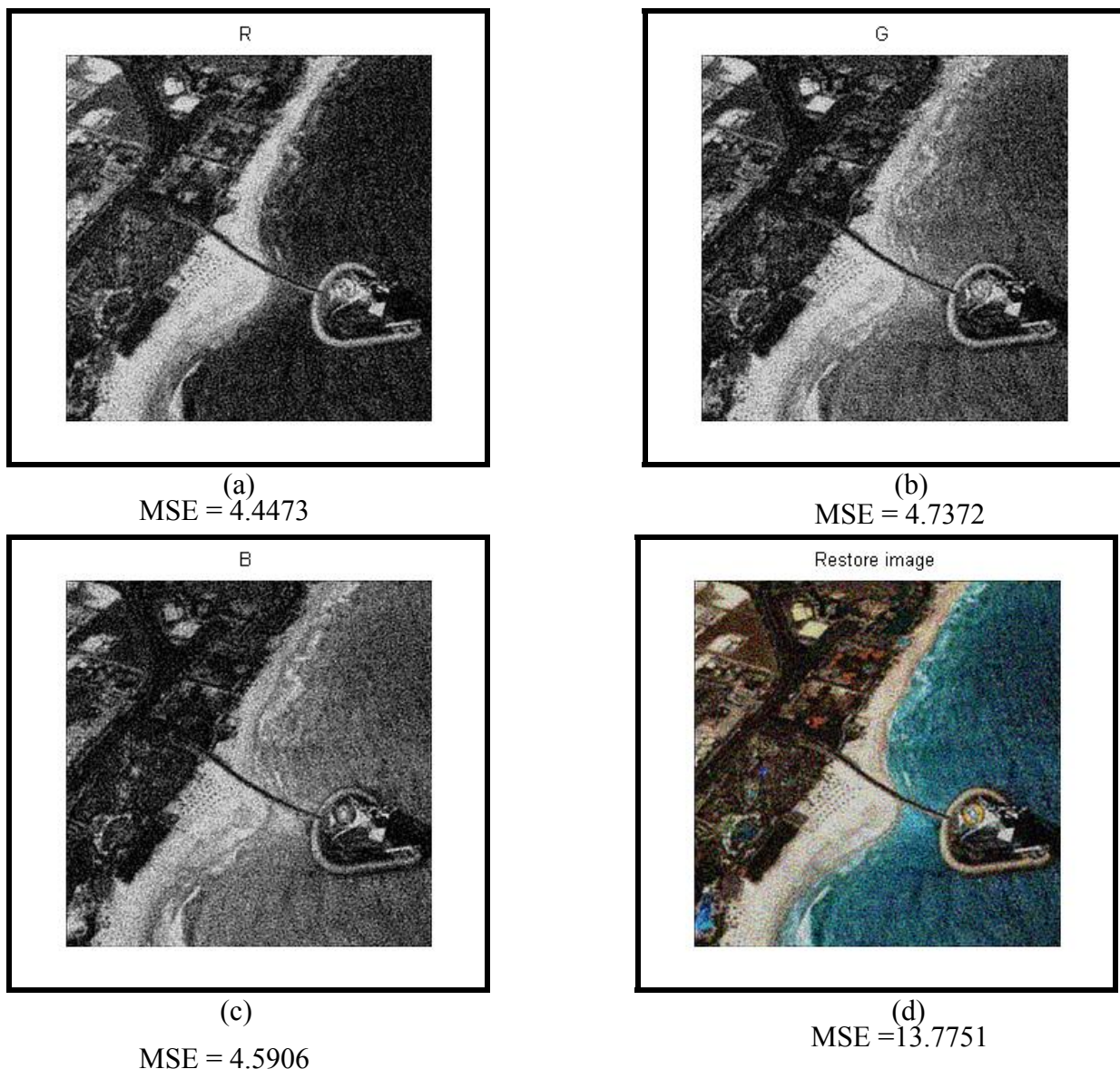
MSE =4.7918

Figure(3-18) Restored Image
for red, green , blue components of image and RGB image respectively.

2. Wiener Filter

Figure (3-19) represent the restored image of the degraded image with Gaussian Point Spread Function and Gaussian noise, with $\sigma = 0.5$, and SNR=5.

a : represent the restored image for red component, b: represent the restored image for green component, c: represent the restored image for blue component, and d: represent the restored image for RGB image ,using Wiener filter. The figure shows, also, the (MSE) of the degraded image with respect to the original image.



Figure(3-19) Restored Image for red, green , blue components of image and RGB image respectively.

Figure (3-20) represent the restored image of the degraded image with Gaussian Point Spread Function and Gaussian noise, with $\sigma = 0.5$, and SNR=20. a : represent the restored image for red component, b: represent the restored image for green component, c: represent the restored image for blue component, and d: represent the restored image for RGB image , using Wiener filter. The figure shows, also, the (MSE) of the degraded image with respect to the original image.

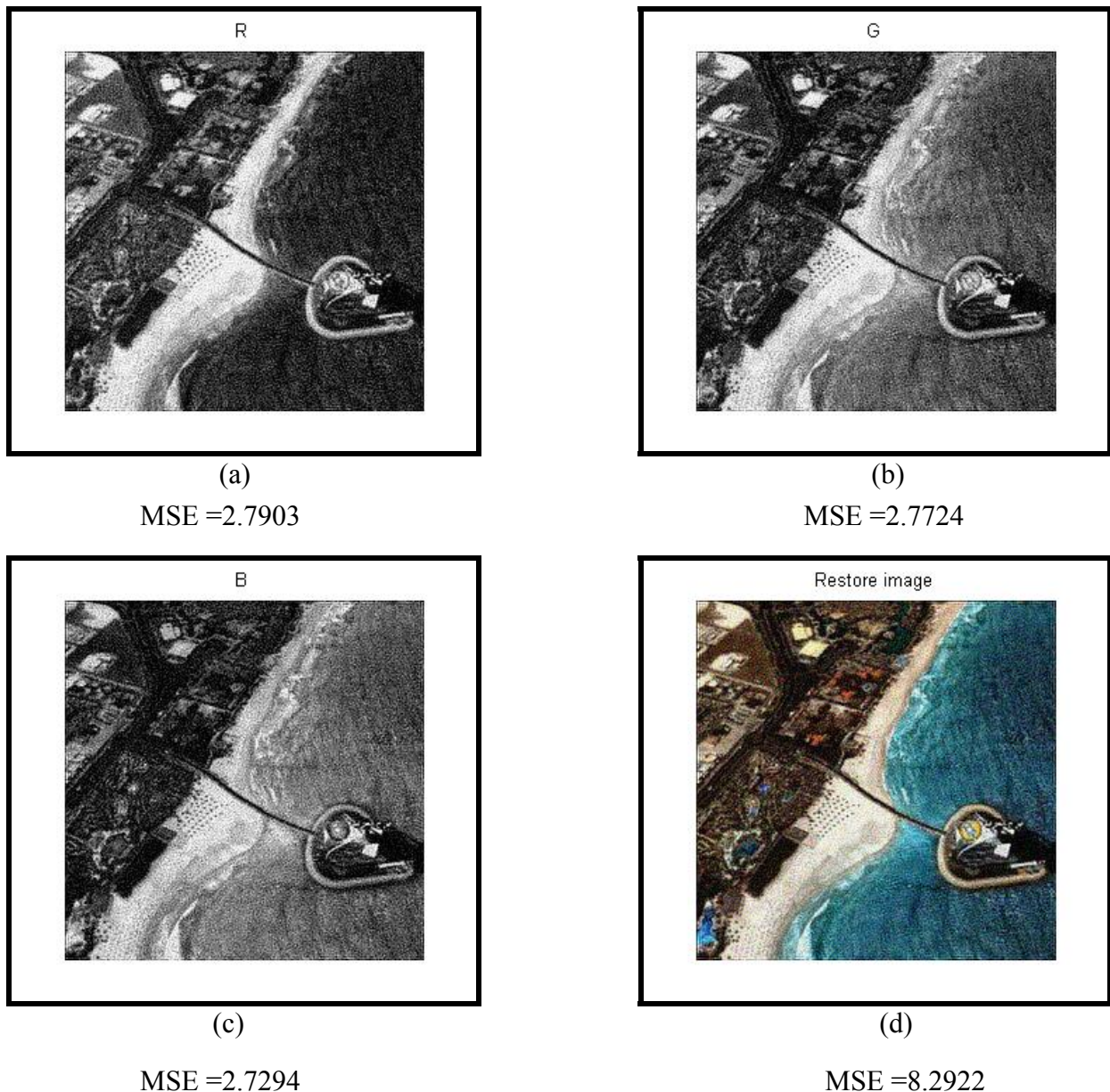
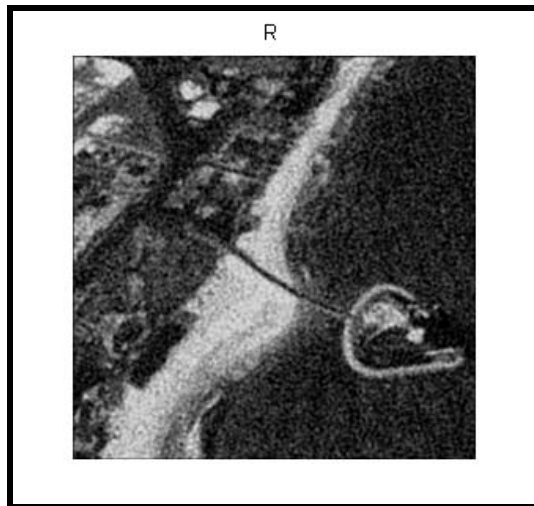


Figure (3-20) Restored Image for red, green , blue components of image and RGB image respectively.

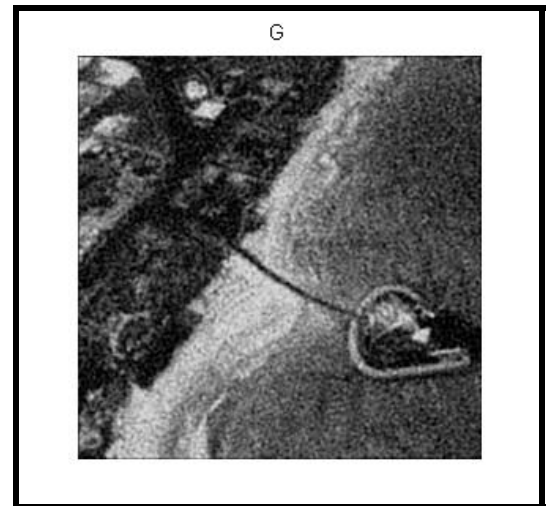
Figure (3-21) represent the restored image of the degraded image with Gaussian Point Spread Function and Gaussian noise, with $\sigma = 1$, and SNR=5.

a : represent the restored image for red component, b: represent the restored image for green component, c: represent the restored image for blue component, and d: represent the restored image for RGB image ,using Wiener filter. The figure shows, also, the (MSE) of the degraded image with respect to the original image.



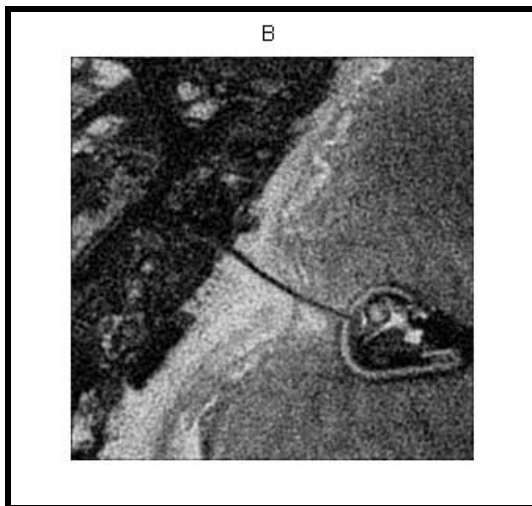
(a)

MSE =4.1306



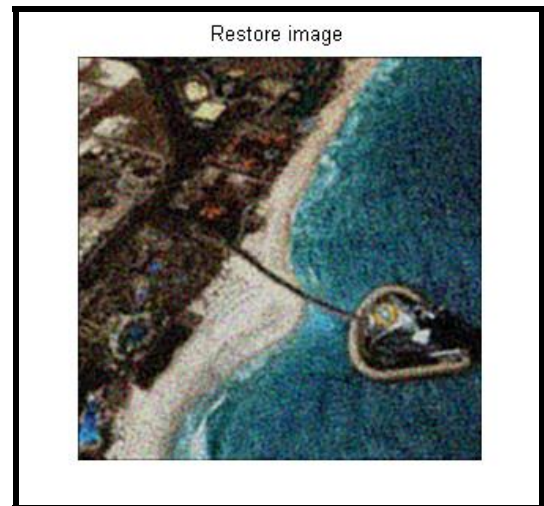
(b)

MSE =4.3622



(c)

MSE =4.1962

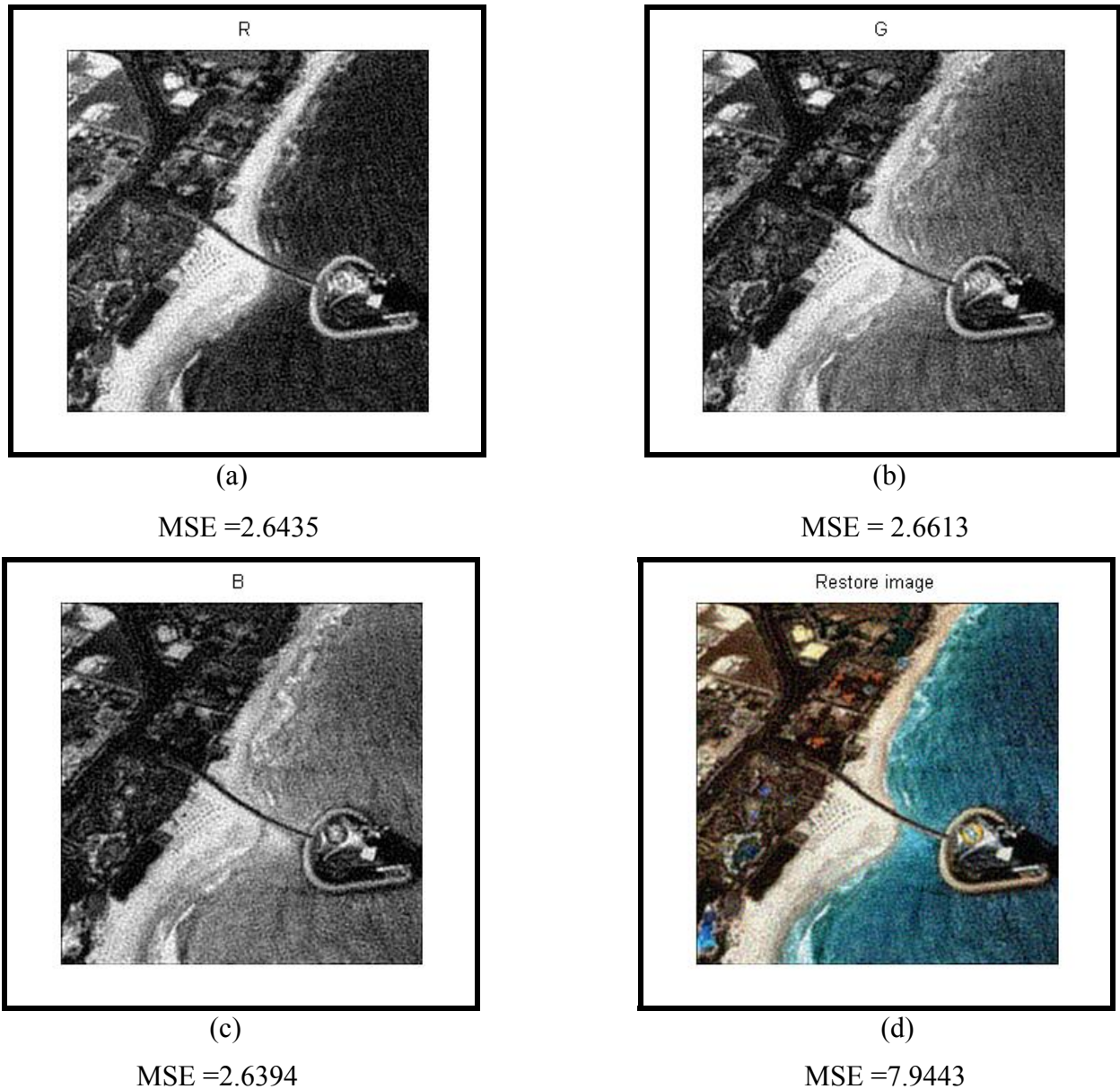


(d)

MSE =12.6890

Figure(3-21) Restored Image
for red, green , blue components of image and RGB image respectively.

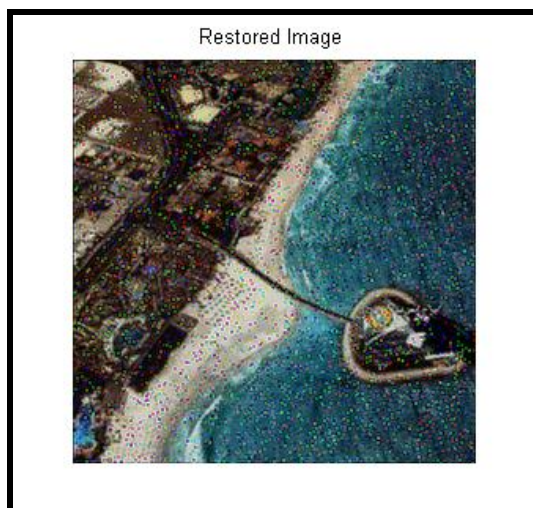
Figure (3-22) represent the restored image of the degraded image with Gaussian Point Spread Function and Gaussian noise, with $\sigma = 1$, and SNR=20. a : represent the restored image for red component, b: represent the restored image for green component, c: represent the restored image for blue component, and d: represent the restored image for RGB image , using Wiener filter. The figure shows, also, the (MSE) of the degraded image with respect to the original image.



Figure(3-22) Restored Image for red, green , blue components of image and RGB image respectively.

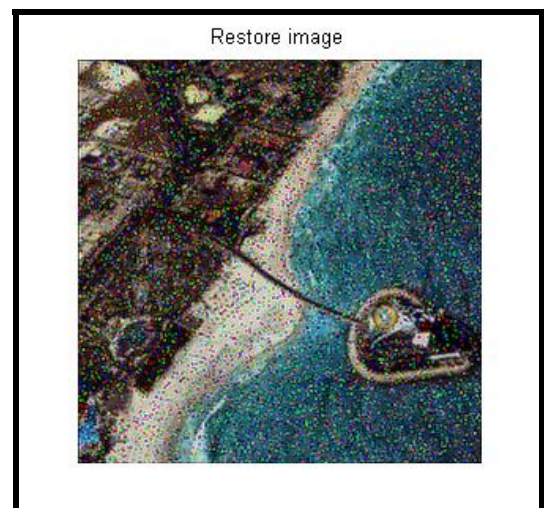
Figure (3-23) represent the restored image of the degraded image with Gaussian Point Speared Function and Salt and Pepper noise, with different parameter , where

a : represent the restored image of the degraded image with $\sigma = 0.5$ and $d=0.05$,
 b: represent the restored image of the degraded image with $\sigma = 0.5$,and $d=0.1$,
 c: represent the restored image of the degraded image with $\sigma = 1$,and $d=0.05$,
 d: represent the restored image of the degraded image with $\sigma = 1$,and $d=0.1$,
 using Wiener filter. The figure shows, also, the (MSE) of the degraded image with respect to the original image.



(a)

MSE =16.8919



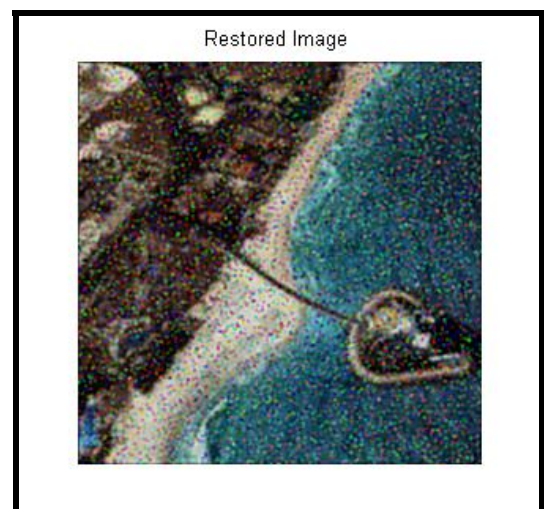
(b)

MSE =26.7891



(c)

MSE =14.3029



(d)

MSE =18.7674

Figure(3-23) Restored Image

3. Constrained Least-Squares Filter (Regular Filter)

Figure (3-24) represent the restored image of the degraded image with Gaussian Point Speared Function and Gaussian noise, with different parameter , where

a : represent the restored image of the degraded image with $\sigma = 0.5$ and SNR =5,

b: represent the restored image of the degraded image with $\sigma = 0.5$ and SNR =20,

c : represent the restored image of the degraded image with $\sigma = 1$ and SNR =5,

d: represent the restored image of the degraded image with $\sigma = 1$ and SNR =20, using Constrained Least-Squares Filter. The figure shows, also, the (MSE) of the degraded image with respect to the original image.



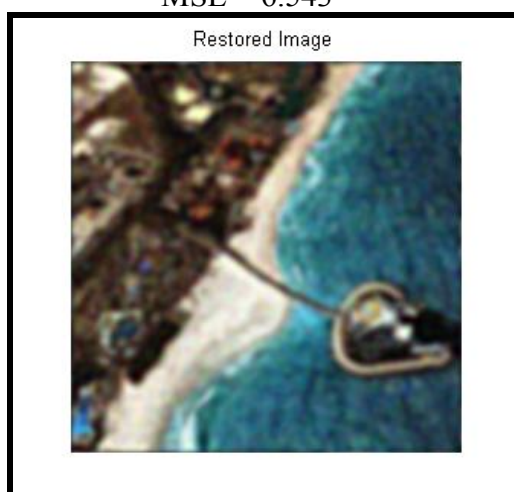
(a)

MSE = 6.543



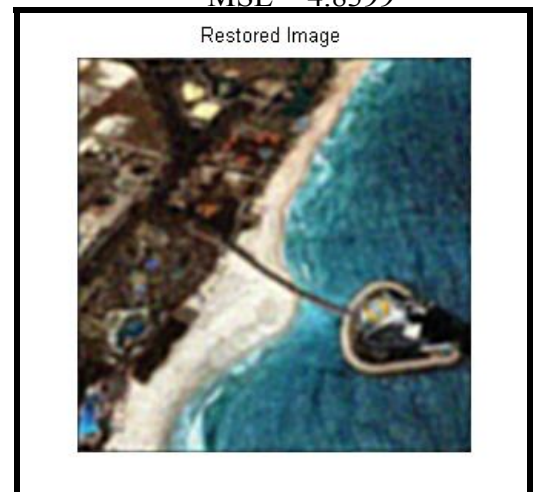
(b)

MSE = 4.8399



(c)

MSE =9.1764



(d)

MSE =6.5621

Figure(3-24) Restored Image

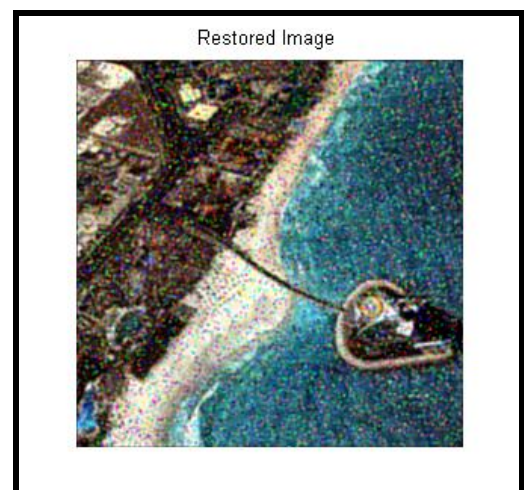
Figure (3-25) represent the restored image of the degraded image with Gaussian Point Spread Function and Salt and Pepper noise, with different parameter , where

a : represent the restored image of the degraded image with $\sigma = 0.5$ and $d=0.05$,
 b: represent the restored image of the degraded image with $\sigma = 0.5$,and $d=0.1$,
 c: represent the restored image of the degraded image with $\sigma = 1$,and $d=0.05$,
 d: represent the restored image of the degraded image with $\sigma = 1$,and $d=0.1$,
 using Constrained Least-Squares Filter.

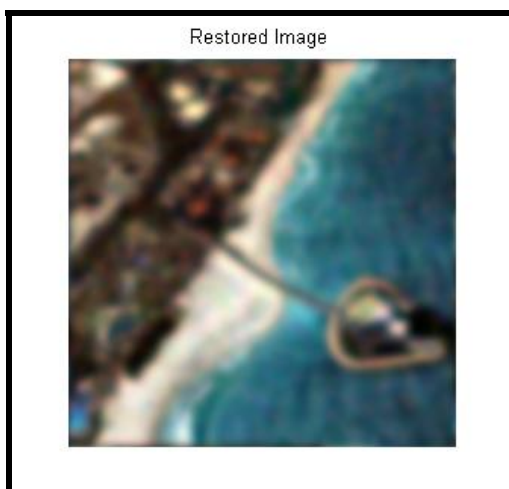
The figure shows, also, the (MSE) of the degraded image with respect to the original image.



(a)
MSE = 7.2833



(b)
MSE = 12.6894



(c)
MSE = 12.1251



(d)
MSE = 10.1128

Figure(3-25) Restored Image

4. Iterative Restoration(Tikhonov method)

Figure (3-26a) represent the restored image of the degraded image with Gaussian Point Speared Function and Gaussian noise, with $\sigma = 0.5$,and SNR=5.

This figure represent the restored image for RGB image after 6 iterations, using Tikhonov method. when $\alpha = 0$.



MSE =9.6277

Figure(3-26a) Restored image for RGB image after 6 iterations

Figure (3-26b) represent MSE Versus no. of iterations for the restored image of the degraded image with Gaussian Point Speared Function and Gaussian noise, with $\sigma = 0.5$,and SNR=5. For red, green, blue components, and RGB image , using Iterative Restoration When $\alpha =0$.

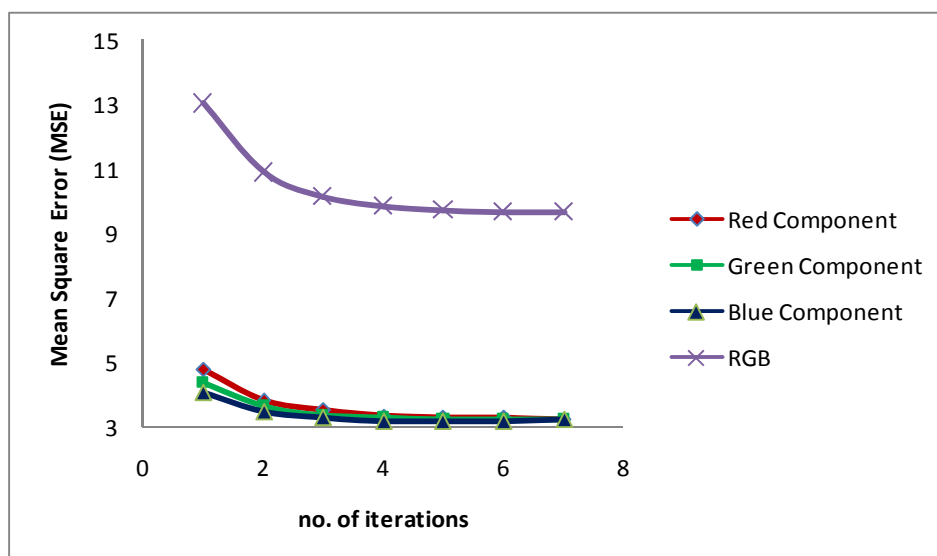


Figure (3-26b)
MSE Versus. no. of iterations

Figure (3-27a) represent the restored image of the degraded image with Gaussian blur and Gaussian noise, with $\sigma = 0.5$, and SNR=20 for RGB image, using Tikhonov method after 7 iterations. when $\alpha = 0$ (α : regularization parameter).

Figure (3-27b) represent MSE Versus no. of iterations.

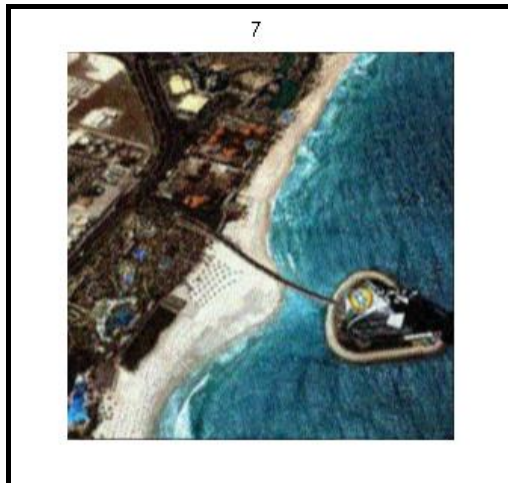


Figure (3-27a)
MSE = 7.07
Restored image for RGB image after
7 iterations

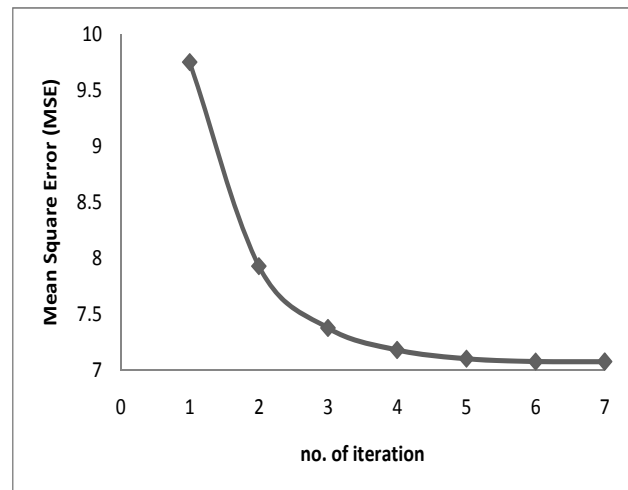


Figure (3-27b)
MSE Versus no. of iterations when degraded
image with $\sigma = 0.5$, and SNR=20

Figure (3-28a) represent the restored image of the degraded image with Gaussian blur and Gaussian noise, with $\sigma = 1$, and SNR=5 for RGB image, using Tikhonov method after 10 iterations. when $\alpha = 0$ (α : regularization parameter).

Figure (3-28b) represent MSE Versus no. of iterations.

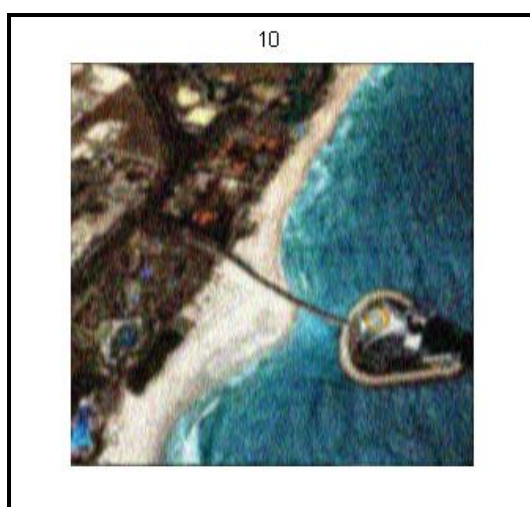


Figure (3-28a)
MSE = 9.86
Restored image for RGB image after
10 iterations

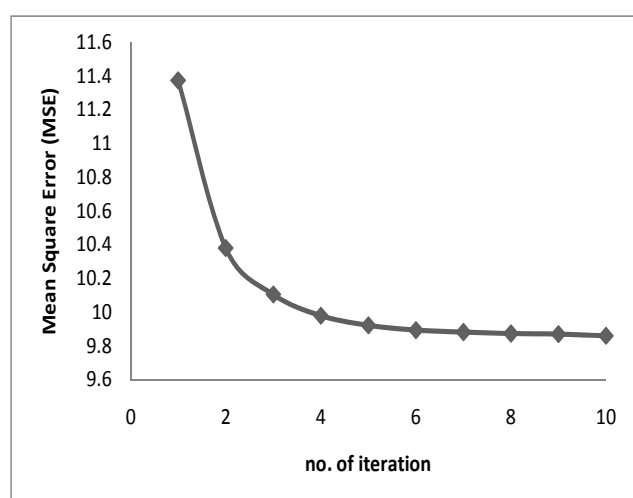


Figure (3-28b)
MSE VS. no. of iterations when degraded
image with $\sigma = 1$, and SNR=5

Figure (3-29a) represent the restored image of the degraded image with Gaussian blur and Gaussian noise, with $\sigma = 1$, and SNR=20 for RGB image, using Tikhonov method after 30 iterations. when $\alpha = 0$ (α : regularization parameter).

Figure (3-29b) represent MSE Versus no. of iterations.



Figure (3-29a)

MSE = 8.11

Restored image for RGB image after 30 iterations

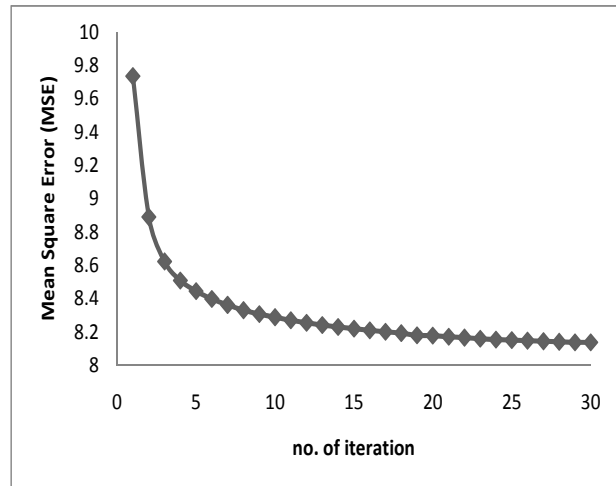


Figure (3-29b)

MSE VS. no. of iterations when degraded image with $\sigma = 1$, and SNR=20

Figure (3-30a) represent the restored image of the degraded image with Gaussian blur and Salt and pepper noise, with $\sigma = 0.5$, and $d=0.05$ for RGB image, using Tikhonov method after 4 iterations. when $\alpha = 0$ (α : regularization parameter).

Figure (3-30b) represent Mean Square Error (MSE) Versus no. of iterations.

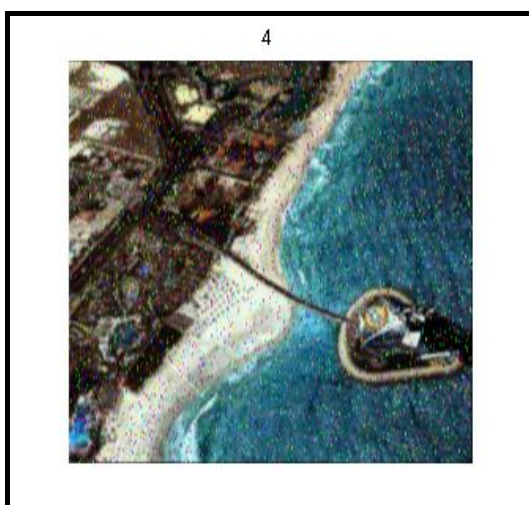


Figure (3-30a)

MSE = 11.209

Restored image for RGB image after 4 iterations

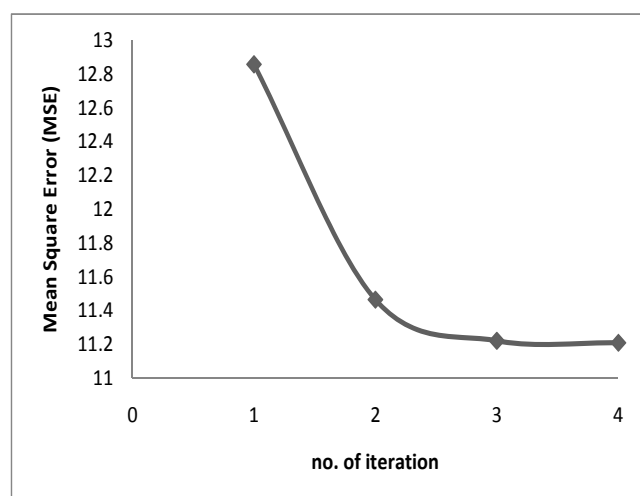


Figure (3-30b)

MSE VS. no. of iterations when degraded image with $\sigma = 0.5$, and $d=0.05$

Figure (3-31a) represent the restored image of the degraded image with Gaussian blur and Salt and pepper noise, with $\sigma = 0.5$,and $d=0.1$ for RGB image , using Tikhonov method after 4 iterations. when $\alpha = 0$ (α : regularization parameter).

Figure (3-31b) represent MSE Versus no. of iterations .



Figure (3-31a)
MSE = 15.921
Restored image for RGB image after 4 iterations

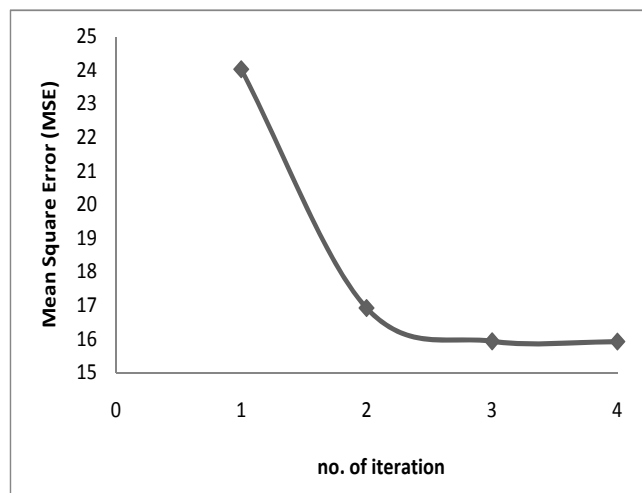


Figure (3-31b)
MSE VS. no. of iterations when degraded image with $\sigma =0.5$, and $d=0.1$

Figure (3-32a) represent the restored image of the degraded image with Gaussian blur and Salt and pepper noise, with $\sigma = 1$,and $d=0.05$ for RGB image , using Tikhonov method after 5 iterations. when $\alpha = 0$ (α : regularization parameter). Figure (3-32b) represent MSE Versus no. of iterations .

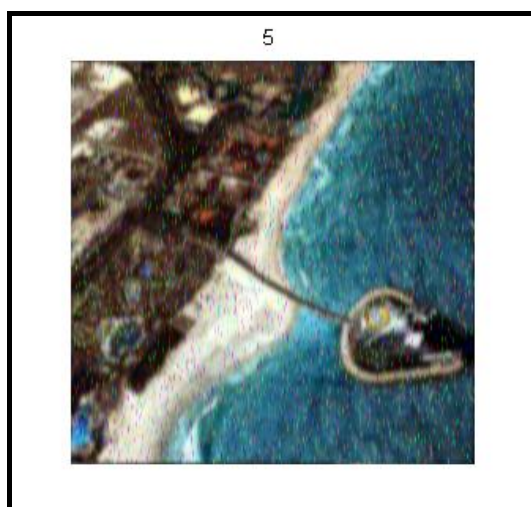


Figure (3-32a)
MSE = 11.071
Restored image for RGB image after 5 iterations

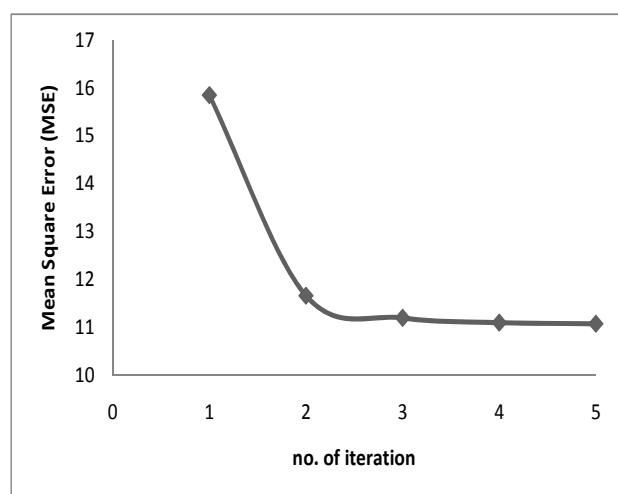


Figure (3-32b)
MSE VS. no. of iterations when degraded image with $\sigma =1$, and $d=0.05$

Figure (3-33a) represent the restored image of the degraded image with Gaussian blur and Salt and pepper noise, with $\sigma = 1$,and $d=0.1$ for RGB image , using Tikhonov method after 3 iterations. when $\alpha = 0$ (α : regularization parameter)

Figure (3-33b) represent MSE Versus no. of iterations .

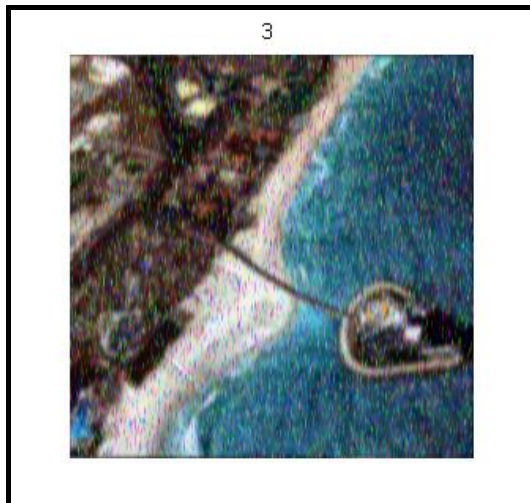


Figure (3-33a)

MSE = 14.21

Restored image for RGB image after 3 iterations

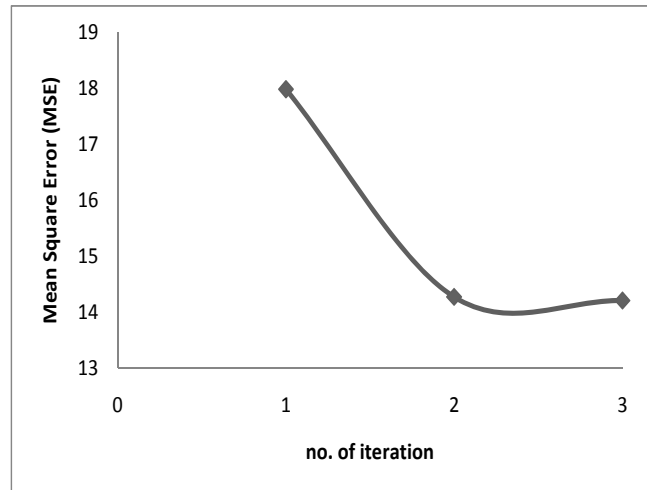


Figure (3-33b)

MSE VS. no. of iterations when degraded image with $\sigma = 1$, and $d=0.1$

Figure (3-34a) represent the restored image of the degraded image with Gaussian blur and Salt and pepper noise, with $\sigma = 2$,and $d=0.05$ for RGB image , using Tikhonov method after 17 iterations. When $\alpha = 0$ (α : regularization parameter)

Figure (3-34b) represent MSE Versus no. of iterations .



Figure (3-34a)

MSE =13.294

Restored image for RGB image after 17 iterations

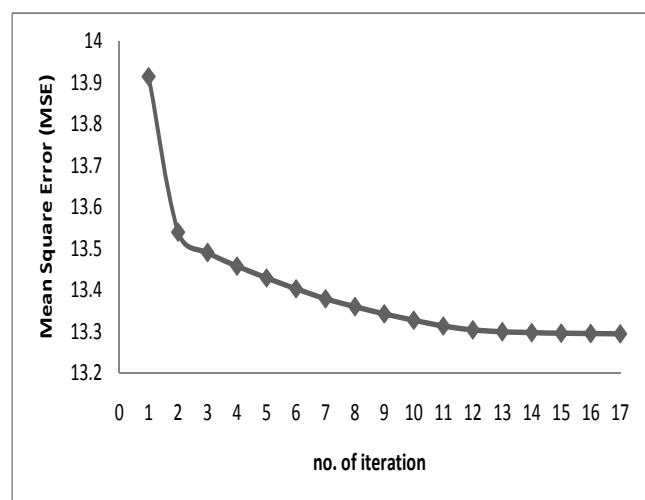


Figure (3-34b)

MSE VS. no. of iterations when degraded image with $\sigma = 2$, and $d=0.05$

Figure (3-35a) represent the restored image of the degraded image with Gaussian blur and Gaussian noise, with $\sigma = 0.5$,and SNR=5 for RGB image , using Tikhonov method after 7 iterations. when $\alpha = 0.5$ (α : regularization parameter).

Figure (3-35b) represent MSE Versus no. of iterations .

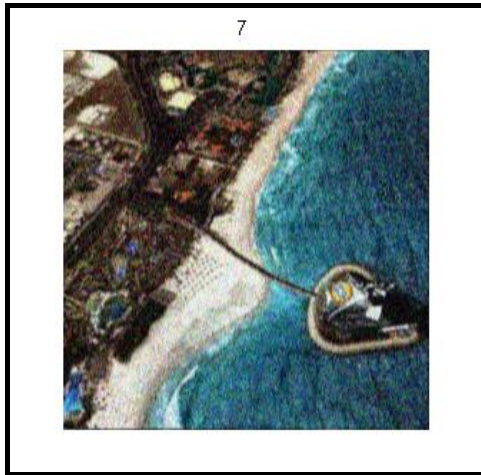


Figure (3-35a)

MSE = 9.7

Restored image for RGB image after 7 iterations

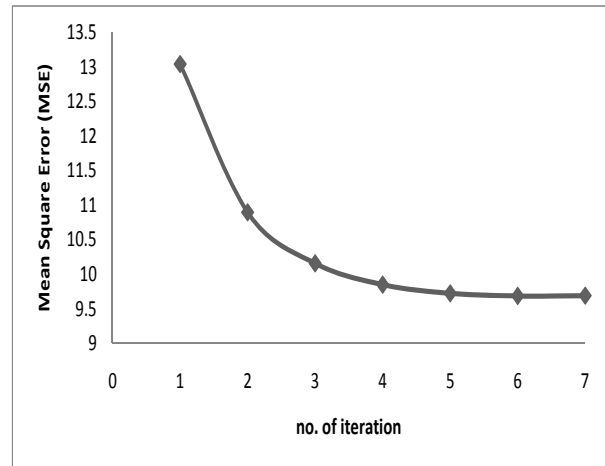


Figure (3-35b)

MSE VS. no. of iterations when degraded image with $\sigma =0.5$,and SNR=5

Figure (3-36a) represent the restored image of the degraded image with Gaussian blur and Gaussian noise, with $\sigma = 0.5$,and SNR=20 for RGB image , using Tikhonov method after 8 iterations. when $\alpha = 0.5$ (α : regularization parameter).

Figure (3-36b) represent MSE Versus no. of iterations .



Figure (3-36a)

MSE = 7.1264

Restored image for RGB image after 8 iterations

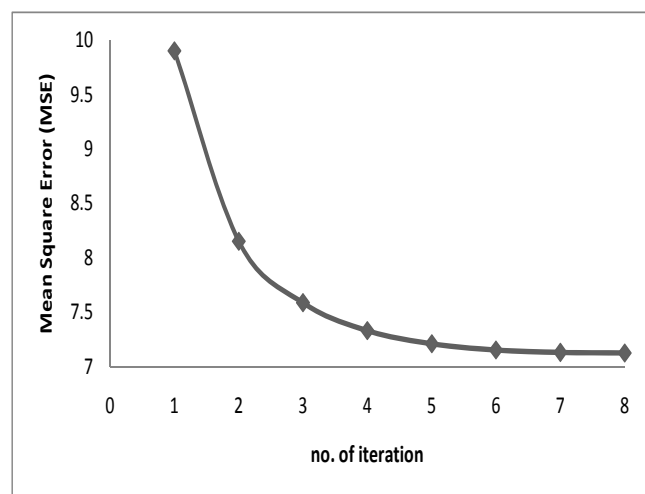


Figure (3-36b)

MSE VS. no. of iterations when degraded image with $\sigma =0.5$, and SNR=20

Figure (3-37a) represent the restored image of the degraded image with Gaussian blur and Gaussian noise, with $\sigma = 1$,and SNR=5 for RGB image , using Tikhonov method after 9 iterations. when $\alpha = 0.5$ (α : regularization parameter).

Figure (3-37b) represent MSE Versus no. of iterations .

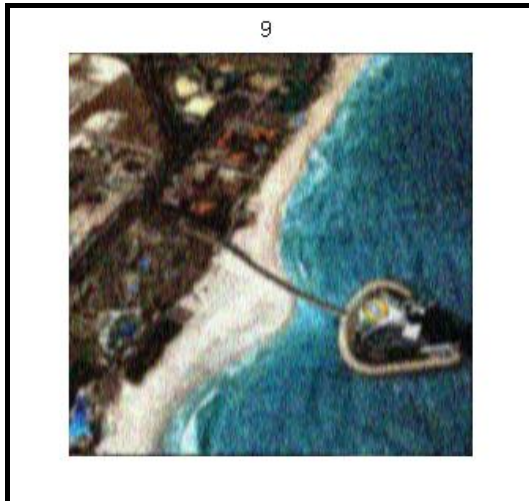


Figure (3-37a)
MSE = 9.8214
Restored image for RGB image after 9 iterations

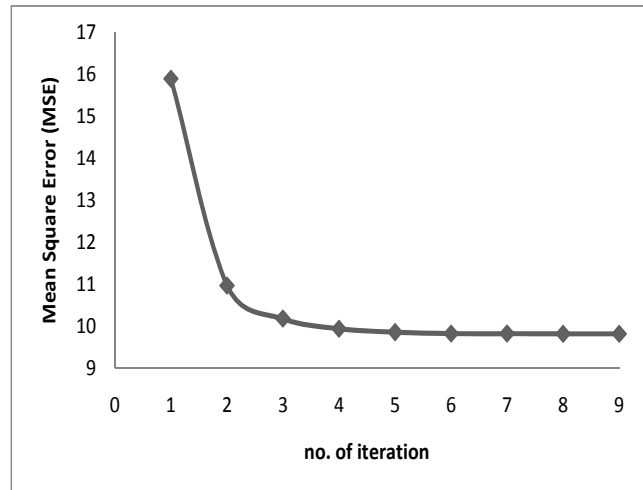


Figure (3-37b)
MSE VS. no. of iterations when degraded image with σ , and SNR=5

Figure (3-38a) represent the restored image of the degraded image with Gaussian blur and Gaussian noise, with $\sigma = 1$,and SNR=20 for RGB image , using Tikhonov method after 30 iterations. when $\alpha = 0$ (α : regularization parameter).

Figure (3-38b) represent MSE Versus no. of iterations .



Figure (3-38a)
MSE = 8.155
Restored image for RGB image after 30 iterations

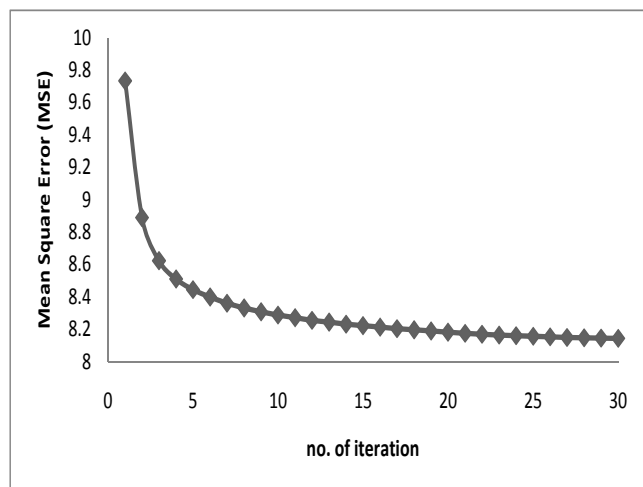


Figure (3-38b)
MSE VS. no. of iterations when degraded image with $\sigma = 1$, and SNR=20

Figure (3-39a) represent the restored image of the degraded image with Gaussian blur and Salt and pepper noise, with $\sigma = 0.5$,and $d=0.05$ for RGB image ,using Tikhonov method after 4 iterations. when $\alpha = 0.5$ (α : regularization parameter). Figure (3-39b) represent MSE Versus no. of iterations .



Figure (3- 39a)
MSE = 10.9595
Restored image for RGB image after 4 iterations

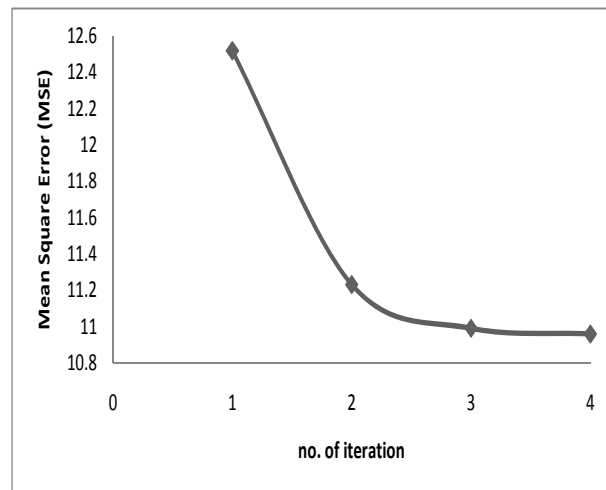


Figure (3-39b)
MSE VS. no. of iterations when degraded image with $\sigma =0.5$, and $d=0.05$

Figure (3-40a) represent the restored image of the degraded image with Gaussian blur and Salt and pepper noise, with $\sigma = 0.5$,and $d=0.1$ for RGB image , using Tikhonov method after 4 iterations. when $\alpha = 0.5$ (α : regularization parameter). Figure (3-40b) represent MSE Versus no. of iterations .



Figure (3-40a)
MSE = 15.32061
Restored image for RGB image after 4 iterations

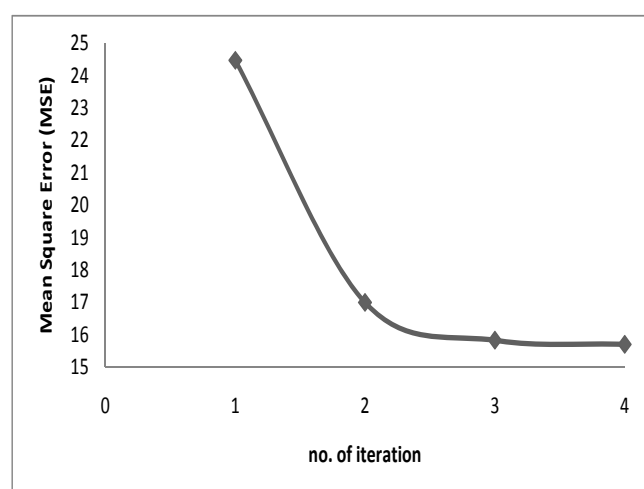


Figure (3- 40b)
MSE VS. no. of iterations when degraded image with $\sigma =0.5$, and $d=0.1$

Figure (3-41a) represent the restored image of the degraded image with Gaussian blur and Salt and pepper noise, with $\sigma = 1$, and $d=0.05$ for RGB image, using Tikhonov method after 5 iterations. when $\alpha = 0.5$ (α : regularization parameter). Figure (3-41b) represent MSE Versus no. of iterations.

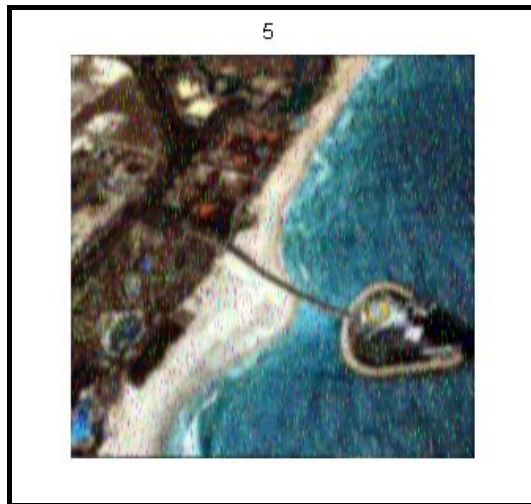


Figure (3-41a)

MSE = 10.78

Restored image for RGB image after 5 iterations

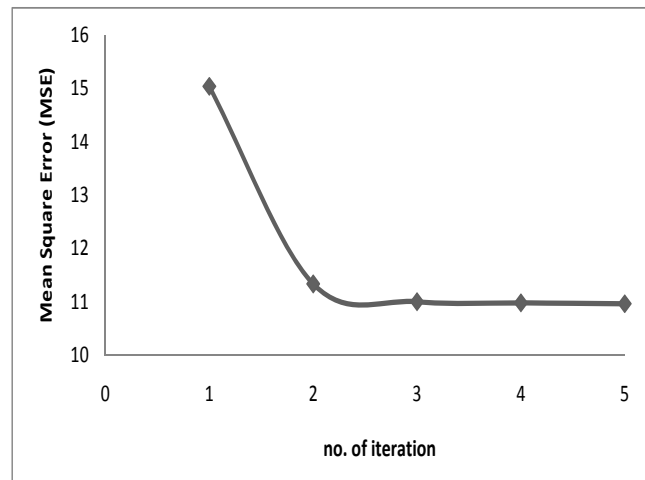


Figure (3-41b)

MSE VS. no. of iterations when degraded image with $\sigma = 1$, and $d=0.05$

Figure (3-42a) represent the restored image of the degraded image with Gaussian blur and Salt and pepper noise, with $\sigma = 1$, and $d=0.1$ for RGB image, using Tikhonov method after 3 iterations. when $\alpha = 0.5$ (α : regularization parameter). Figure (3-42b) represent MSE Versus no. of iterations.

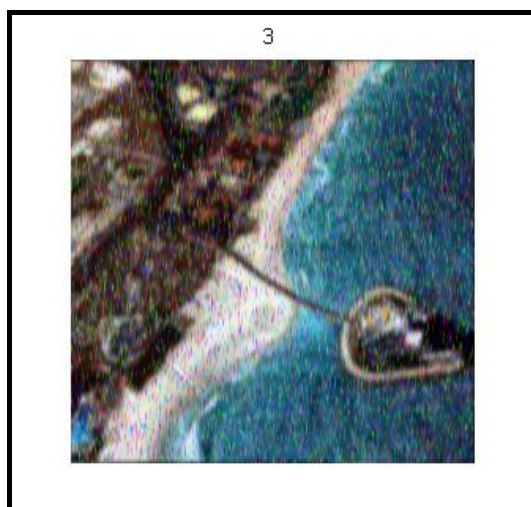


Figure (3-42a)

MSE = 14.0196

Restored image for RGB image after 3 iterations

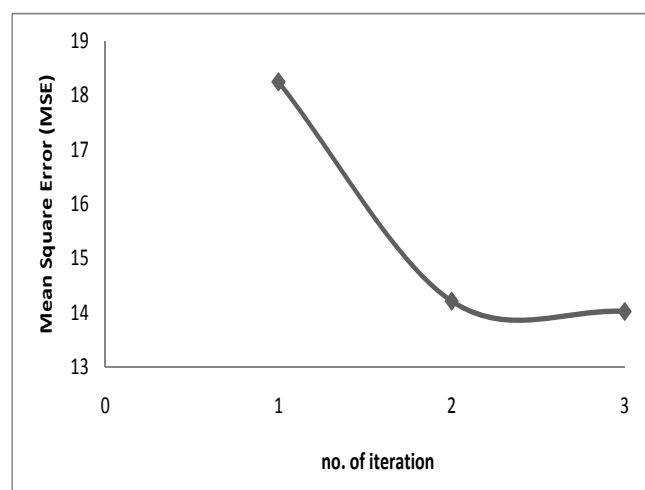


Figure (3-42b)

MSE VS. no. of iterations when degraded image with $\sigma = 1$, and $d=0.1$

Figure (3-43) represent MSE Versus no. of iterations for restored image of degraded image with Gaussian Point Speared Function and Gaussian noise, with $\sigma = 0.5$, and SNR=5. when $\alpha = 0.5$, and $\alpha = 0$.

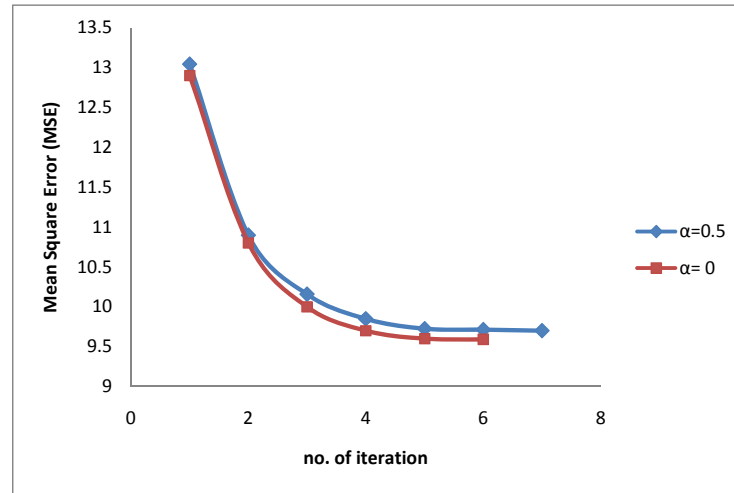


Figure (3- 43)
MSE VS. no. of iteration
when degraded image with Gaussian PSF and
Gaussian noise with $\sigma =0.5$, and SNR =5

Figure (3-44) represent MSE Versus no. of iterations for restored image of degraded image with Gaussian Point Speared Function and Gaussian noise, with $\sigma = 0.5$, and SNR=10. when $\alpha = 0.5$, and $\alpha = 0$.

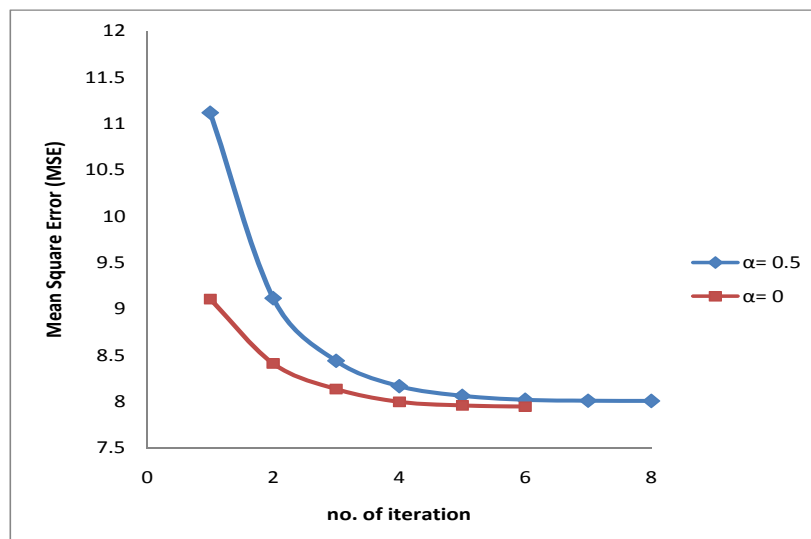


Figure (3- 44)
MSE VS. no. of iteration
when degraded image with Gaussian PSF and Gaussian
noise with $\sigma =0.5$, and SNR =10

Figure (3-45) represent MSE Versus no. of iterations for restored image of degraded image with Gaussian Point Speared Function and Gaussian noise, with $\sigma = 0.5$, and SNR=20. when $\alpha = 0.5$, and $\alpha = 0$.

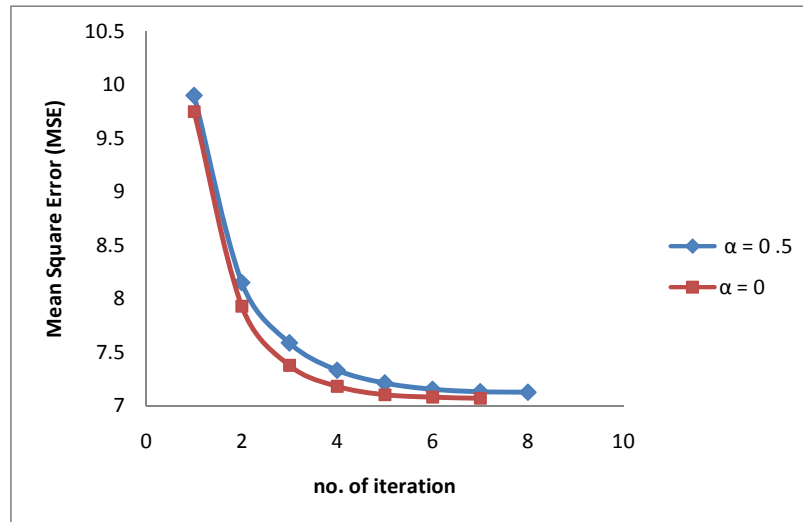


Figure (3- 45)
Mean Square Error VS. no. of iteration
when degraded image with Gaussian PSF and Gaussian
noise with $\sigma = 0.5$, and SNR =20

Figure (3-46) represent MSE Versus no. of iterations for restored image of degraded image with Gaussian Point Speared Function and Gaussian noise, with $\sigma = 1$, and SNR=5. when $\alpha = 0.5$, and $\alpha = 0$.

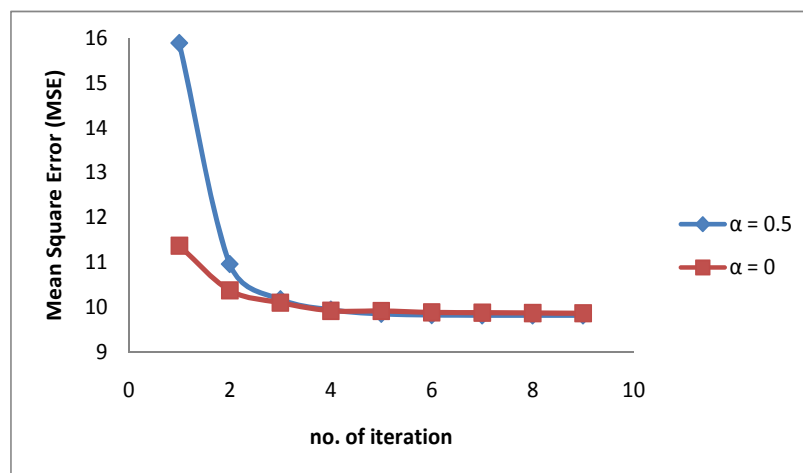


Figure (3- 46)
MSE VS. no. of iteration
when degraded image with Gaussian PSF and Gaussian
noise with $\sigma = 1$, and SNR =5

Figure (3-47) represent MSE Versus no. of iterations for restored image of degraded image with Gaussian Point Speared Function and Gaussian noise, with $\sigma = 1$, and SNR=10. when $\alpha = 0.5$, and $\alpha = 0$.

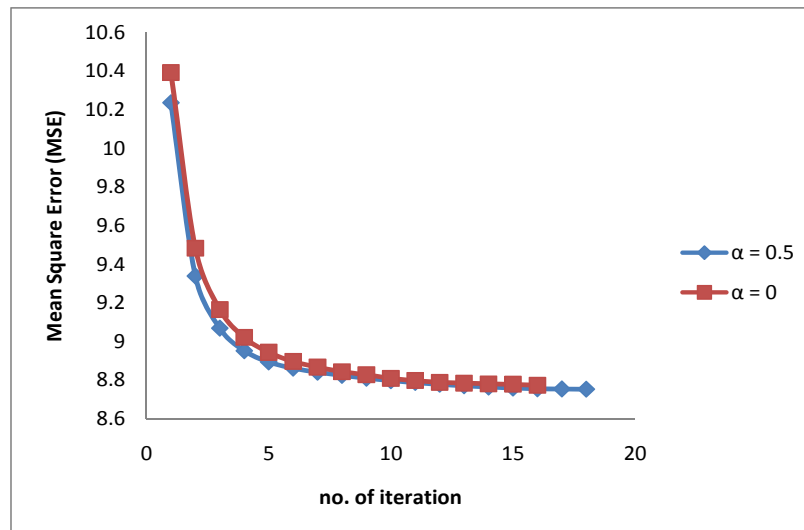


Figure (3- 47)
MSE VS. no. of iteration
when degraded image with Gaussian PSF and Gaussian
noise with $\sigma =1$,and SNR =10

Figure (3-48) represent MSE Versus no. of iterations for restored image of degraded image with Gaussian Point Speared Function and Gaussian noise, with $\sigma = 1$, and SNR=20. when regularization parameter " α ", $\alpha = 0.5$, and $\alpha = 0$.

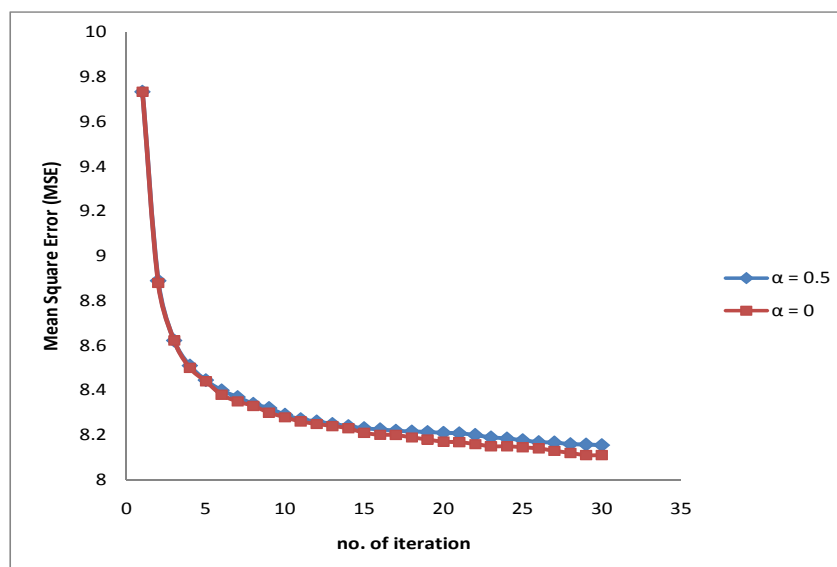


Figure (3- 48)
MSE VS. no. of iteration
when degraded image with Gaussian PSF and Gaussian
noise with $\sigma =1$,and SNR =20

Figure (3-49) represent MSE Versus no. of iterations for restored image of degraded image with Gaussian Point Speared Function and Gaussian noise, with $\sigma = 2$, and SNR=5. when $\alpha = 0.5$, and $\alpha = 0$.

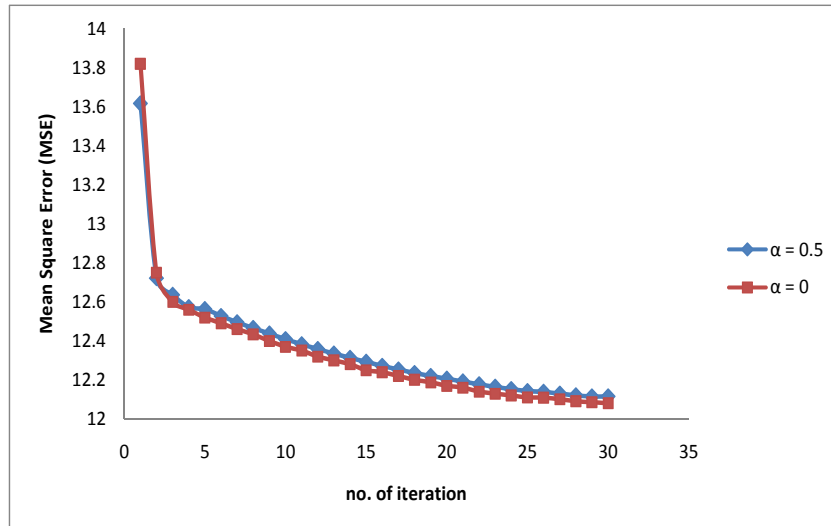


Figure (3- 49)
MSE VS. no. of iteration
when degraded image with Gaussian PSF and Gaussian
noise with $\sigma = 2$, and SNR =5

Figure (3-50) represent MSE Versus no. of iterations for restored image of degraded image with Gaussian Point Speared Function and Gaussian noise, with $\sigma = 2$, and SNR=10. $\alpha = 0.5$, and $\alpha = 0$.

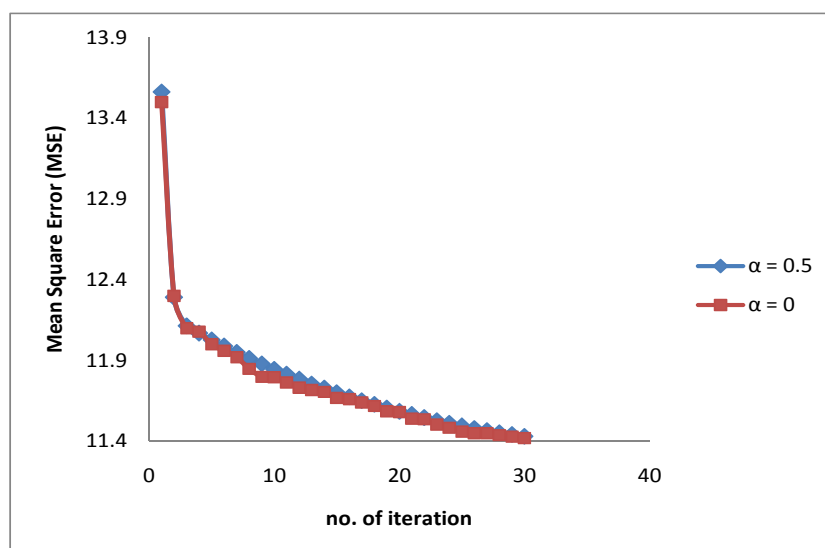


Figure (3- 50)
MSE VS. no. of iteration
when degraded image with Gaussian PSF and Gaussian
noise with $\sigma = 2$, and SNR =10

Figure (3-51) represent MSE Versus no. of iterations for restored image of degraded image with Gaussian Point Speared Function and Gaussian noise, with $\sigma = 2$, and SNR=20. when $\alpha = 0.5$, and $\alpha = 0$.

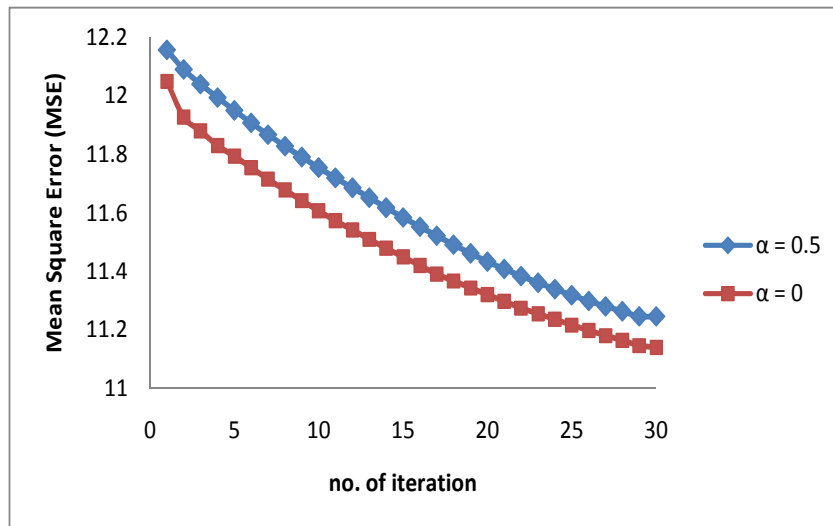


Figure (3- 51)
MSE VS. no. of iterations
when degraded image with Gaussian PSF and Gaussian noise
with $\sigma = 2$, and SNR =20

Figure (3-52) represent MSE Versus no. of iterations for restored image of degraded image with Gaussian Point Speared Function and Salt and Pepper noise, with $\sigma = 0.5$, and $d=0.05$. when $\alpha = 0.5$, and $\alpha = 0$.

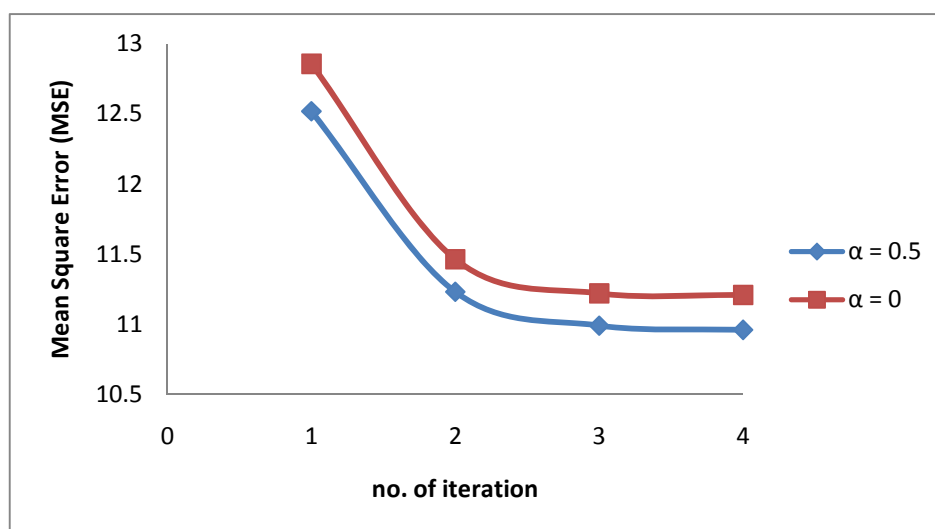


Figure (3- 52)
MSE VS. no. of iteration when degraded image with Gaussian
PSF and Salt and pepper noise with $\sigma = 0.5$, and $d = 0.05$

Figure (3-53) represent MSE Versus no. of iterations for restored image of degraded image with Gaussian Point Speared Function and Salt and Pepper noise, with $\sigma = 0.5$,and $d=0.1$. when $\alpha = 0.5$, and $\alpha = 0$.

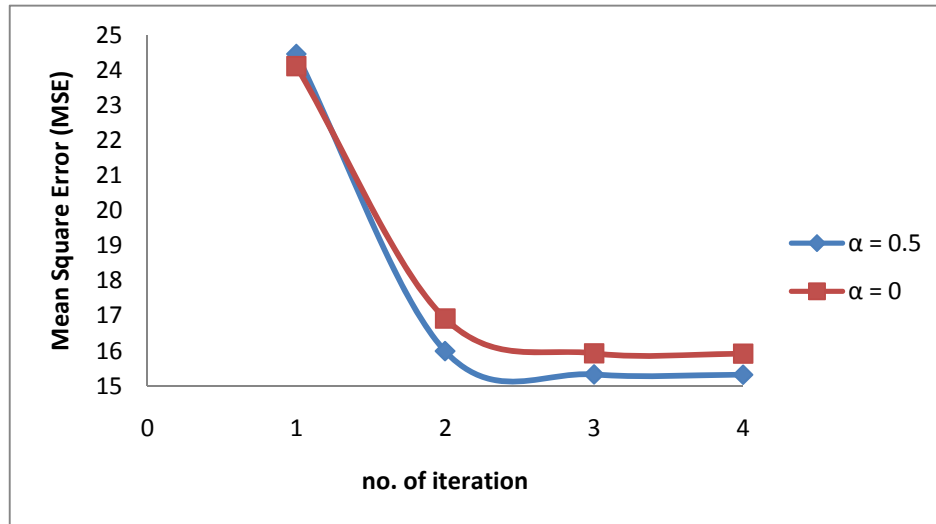


Figure (3- 53)
MSE VS. no. of iterations when degraded image with Gaussian PSF and Salt and pepper noise with $\sigma =0.5$,and $d=0.1$

Figure (3-54) represent MSE Versus no. of iterations for restored image of degraded image with Gaussian Point Speared Function and Salt and Pepper noise, with $\sigma = 1$,and $d=0.05$. when $\alpha = 0.5$, and $\alpha = 0$.

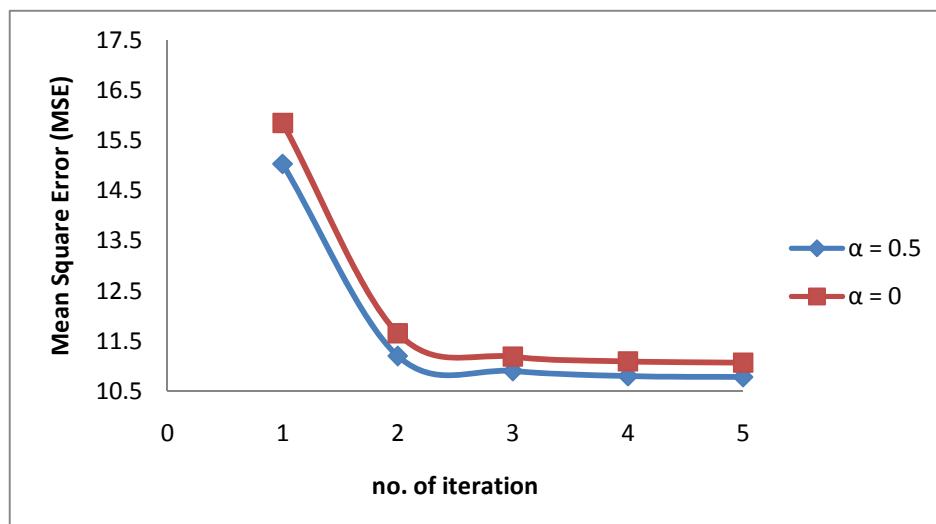


Figure (3-54)
MSE VS. no. of iterations when degraded image with Gaussian PSF and Salt and pepper noise with $\sigma =1$,and $d =0.05$

Figure (3-55) represent MSE Versus no. of iterations for restored image of degraded image with Gaussian Point Speared Function and Salt and Pepper noise, with $\sigma = 1$,and $d=0.1$. when $\alpha = 0.5$, and $\alpha = 0$.

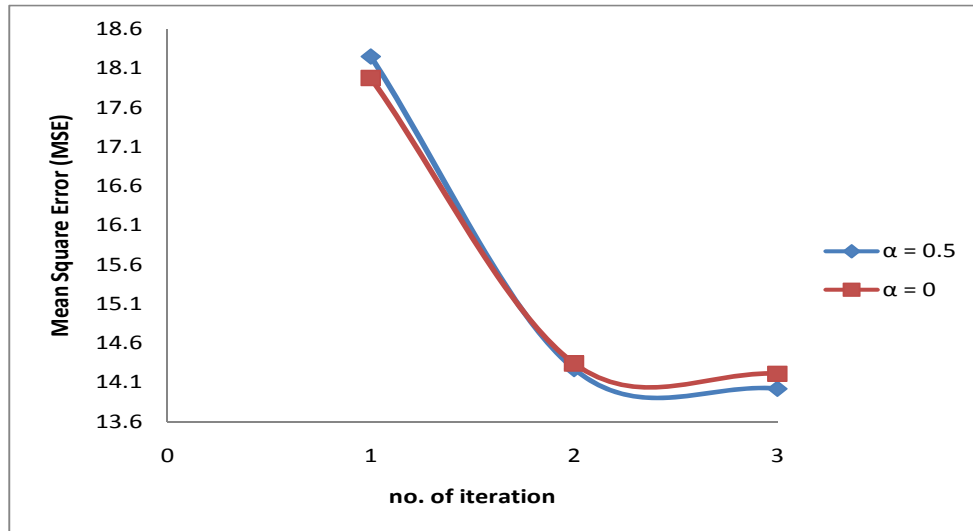


Figure (3- 55)

MSE VS. no. of iterations when degraded image with Gaussian PSF and Salt and pepper noise with $\sigma = 1$,and $d = 0.1$

Figure (3-56) represent MSE Versus no. of iterations for restored image of degraded image with Gaussian Point Speared Function and Salt and Pepper noise, with $\sigma = 2$,and $d=0.05$. when $\alpha = 0.5$, and $\alpha = 0$.

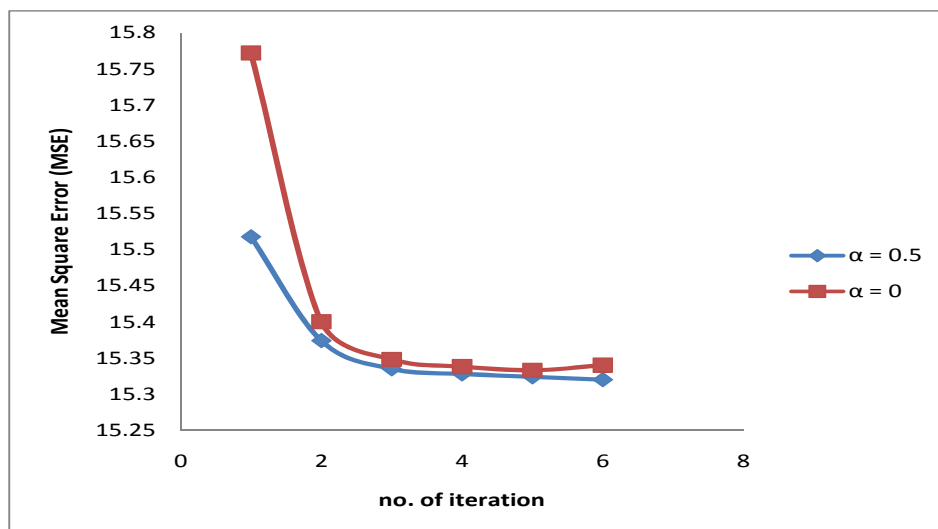


Figure (3- 56)

MSE VS. no. of iterations when degraded image with Gaussian PSF and Salt and pepper noise with $\sigma = 2$,and $d = 0.05$

Figure (3-57) represent MSE Versus no. of iterations for restored image of degraded image with Gaussian Point Speared Function and Salt and Pepper noise, with $\sigma = 2$,and $d=0.1$. when $\alpha = 0.5$, and $\alpha = 0$.

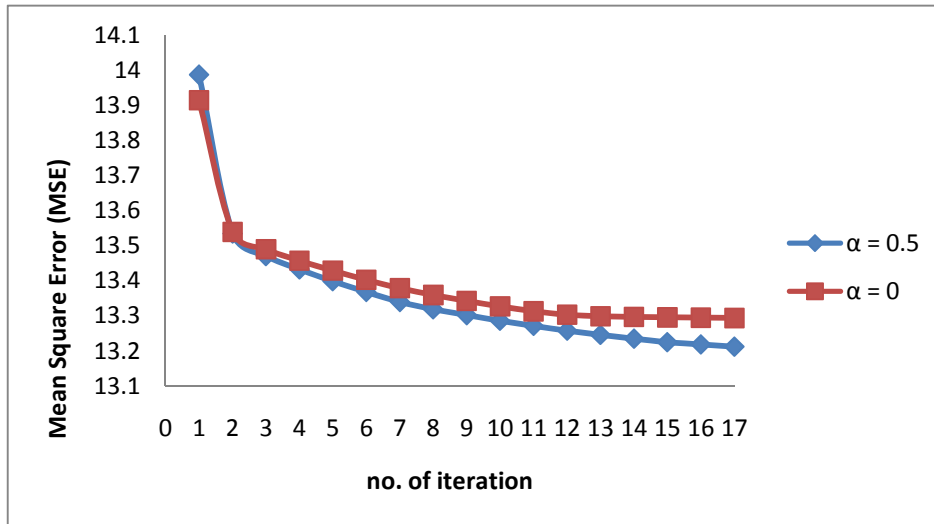


Figure (3- 57)
MSE VS. no. of iterations when degraded image with Gaussian PSF and Salt and pepper noise with $\sigma =2$,and $d =0.1$

3.4 Results Discussion

	σ	SNR=5	SNR=10	SNR=20
		MSE	MSE	MSE
Degraded image	0.5	14.5667	10.4162	8.2159
	1	15.0624	11.059	8.9195
	2	17.4375	13.6742	11.8203
Restored image Using Inverse Filter	0.5	1.8335	1.8335	1.8335
	1	4.7918	4.7918	4.7918
	2	8.6283	8.6283	8.6283
Restored image Using Wiener Filter	0.5	13.7751	10.0890	8.2922
	1	12.6890	9.2262	7.9443
	2	14.6580	10.8900	9.5106
Restored image Using Regular Filter	0.5	6.543	5.9603	4.8399
	1	9.1764	7.5827	6.5621
	2	17.4571	10.0362	9.2042
Restored image Using Tikhonov Filter When $\alpha = 0$	0.5	9.6277 After 6 iterations	7.95 After 6 iterations	7.07 After 7 iterations
	1	9.86 After 10 iterations	8.774 After 16 iterations	8.11 After 30 iterations
	2	12.08 After 30 iterations	11.42 After 30 iterations	11.14 After 30 iterations
Restored image Using Tikhonov Filter When $\alpha = 0.5$	0.5	9.7 After 7 iterations	8.009 After 8 iterations	7.1264 After 8 iterations
	1	9.8214 After 9 iterations	8.753 After 18 iterations	8.155 After 30 iterations
	2	12.115 After 6 iterations	11.4309 After 6 iterations	11.246 After 6 iterations

Table(3-2) shows the MSE of restored images with different type of filter

	σ	d =0.05	d =0.1
		MSE	MSE
Degraded image	0.5	18.74	31.19
	1	19.44	32.26
	2	22.394	34.97
Restored image Using Inverse Filter	0.5	1.8335	1.8335
	1	4.7918	4.7918
	2	8.6283	8.6283
Restored image Using Wiener Filter	0.5	16.8919	26.7891
	1	14.3029	18.7674
	2	15.1719	16.6094
Restored image Using Regular Filter	0.5	7.2833	12.6894
	1	12.1251	10.1128
	2	15.8194	13.1138
Restored image Using Tikhonov Filter When $\alpha = 0$	0.5	11.209 After 4 iterations	15.921 After 4 iterations
	1	11.071 After 5 iterations	14.21 After 3 iterations
	2	13.294 After 17 iterations	15.34 After 6 iterations
Restored image Using Tikhonov Filter When $\alpha = 0.5$	0.5	10.9595 After 4 iterations	15.32061 After 4 iterations
	1	10.78 After 5 iterations	14.0196 After 3 iterations
	2	13.2124 After 17 iterations	15.3245 After 7 iterations

Table(3-2) shows the MSE of restored images with different type of filter.

From the Tables (3-1),and (3-2) can be discussed:

- The degraded (blurred and noisy) images are simulated as follows:

1. The blurred images were simulated by convolving the original image with Gaussian function of different standard deviation ($\sigma = 0.5, 1, \text{ and } 2$), one values of $a = 1$ has been taken.
2. Random noise of Gaussian distribution with zero means was added to the blurred image (obtained in step 1). Different SNR = 5 dB, 10 dB, and 20dB, and noise of salt & pepper distribution with noise density($d = 0.05, \text{ and } 0.1$) was added to the blurred image (obtained in step 1), have been taken.

Figures (3-9),and(3-10),were mean square error vs. SNR and noise density respectively, and show that mean square error its decreased with SNR and increasing with noise density.

To restore the above simulated degraded images,

- The MSE of restored image by using regular filter it is less than Weiner filter and Tikhonov filter , when $\sigma = 2$ and SNR= 5.i.e. when degraded image with high degraded parameters.
- The MSE of restored image by using Tikhonov filter when $\sigma = 2$ and SNR= 5 it is less than other filter except inverse filter.
- The MSE of restored image for corrupted with salt and pepper noise by using regular filter when $\sigma = 2$ and $d=0.05$, it is less than Weiner filter and Tikhonov filter.
- The MSE of restored image for corrupted with salt and pepper noise by using regular filter when $\sigma = 2$ and $d=0.1$, it is less than Weiner filter and Tikhonov filter.
- The values of MSE of restored image by using Tikhonov filter it is different, when $\sigma = 0, \text{ and } a = 0.5$, with different types of noise.
- The number of iterations increased with increasing the degradation parameters.
- Iterative algorithms are normally slow to converge, some of its high computational requirement.



CHAPTER FOUR



***Conclusions
and
Future Work***

4.1 Conclusions

From our results of this research, some notes can be conclude:

1. Tikhonov method was used, the MSE of the restored images decreases with increasing the number of iteration until the result convergence. Also, the ratio of the MSE of the degraded image to the MSE of the restored image will increased with increasing SNR, i.e. this method has better performance for less degradation parameters, with high SNR.
2. The ratio of the MSE of the degraded image (corrupted with salt and pepper noise) to the MSE of the restored image will increased with increasing noise density. This method has better performance for large degradation parameters with high noise density.
3. The Tikhonov methods, causes edge blurring.
4. The values of the regularization parameter (α) depend on the type of the noise.

4.2 Suggest For Future Work

From the work of this research, some notes can be suggested as future work:

1. It is quite interesting for future work, to use a nonlinear technique of image restoration to restore the real an astronomical data and compare results to be obtained with simple technique.
2. Using nonlinear iterative restoration and compare the results with another kind of iterative image restoration. Such as maximum entropy method, POC methods.
3. Using nonlinear iterative restoration with different the relaxation parameter.



References

References

1. **J. Teuber** , " *Digital Image Processing*", First ed., Prentice Hall International(UK)Ltd.(1993).
2. **R. Gonzales** , and **P. Wintz** ," *Digital Image Processing*", Addison-Wesley publishing, (2000).
3. **M. I. Abd - Almajied**," *Image Restoration of Multispectral Satellite Images*", M.Sc. Thesis, University of Baghdad,(2006).
4. **A. Jain** ,"Fundamental of Digital Image Processing", Prentice Hall,(1998).
5. **R. Gonzales, and R. Wood** ," *Digital Image Processing*", Fifth ed., Pearson Education Asia Pte Ltd,(2000).
6. **S. Umbagh** ," *Computer Vision and Image Processing*", Prentice Hall PTR,(1998).
7. **S. A. H. Salih**, "*Theoretical Limits of the Application of an Image Restoration Technique in Astronomy*" ,M.Sc. Thesis, University of Wals,(1983).
8. **N. M. O. Al- Shareefi**, "*Restoration of Astronomical Image Using Adaptive Kalman Filter*", M.Sc. thesis, University of Baghdad,(2000).
9. **A. Rosenfeld, and A. C. Kak**," *Digital Picture Processing* ", Academic Press , Inc,(1976).
10. **W. K. Pratt** ," *Digital Image Processing*", Jhon Wiley & Sons. Inc. Canada, (1978).
11. **D. Angwin, and H.Kaufman**," *Adaptive Restoration of Color Image*", Decision and Control ,Vol. 26, Part 1,1987 Page(s):1196 – 1197.
12. **G. M. P. van Kempen, and L.J. Van Viliy**, "*The influence of the Background Estimation on the Super resolution Properties of Non-Linear Image Restoration* ", Image Acquisition and Processing,vol.6,pp.179-189,(1999)
13. **G. M. P.van Kempen** , and **L.J. Van Viliy**, "*The influence of the Regularization parameter and The First Estimation on the Performance*

References

- of Tikhonov Regularization Non-Linear Image Restoration Algorithms "*,
Journal Of Microscopy,,vol.198,pp.63-75,(2000)
14. **H. Wu, H. J. Zhang, and Z.Liu**, " *Fast Image Restoration in Large Digital Photo*", Digital Object Identifier, Vol. 1, 15-18 ,pp.537 - 540 , (2003).
 15. **S. H. Lee, N. I. Cho, and J.II Park** ,"*Directional Regularization for Constrained Iterative Image Restoration* ", Electronic letters,vol.39 , no.23(2003)
 16. **S. W. Perry, and P. Varjavandi, and L. Guan**, " Adaptive Image Restoration Using a Perception Based Error Measurement", (2004)
www.ewh.ieee.org/reg/7/ccece04/program-weal-vz.pdf.
 17. **Y. H. Chan, and Y. H. Fung**, " *A Regularized Constrained Iterative Restoration Algorithm for Restoring Color Quantized Images*", Signal Processing, vol. 85, pp. 1375- 1387,(2005)
 18. **Q. S. F. Xue, and W. fan** ,"*Iterative Image Restoration Using a non – local Regularization Function and a local Regularization Operator* ", 18 th International Conference on Pattern Recognition ,vol.3,pp.766-769(2006)
 19. **P. Favati, O. Menchi, G. Lotti., and F.Romani** "*Iterative Image Restoration with non negativity Constraints*",(2006)
<http://dienst.isti.cnr.it/dienst/ui/2.0/describe/ercim.cnr.iit/2006-TR-010/tiposearch=cnr=&langre>
 20. **A. Alani**, " *Restoration of Astronomical Image Using an Adaptive Iterative Wiener Filter*", Journal of AL-Nahrain University, College of Science, (2006).
 21. **T. F. Chan, K. Chen, and J. L. Carter**, " *Iterative Methods for Solving the Dual Formulation Arising From Image Restoration*", Electronic Transaction on Numerical Analysis, vol. 26, pp. 299-311,(2007).

References

22. **W. Zhao, A. Pope,** " *Image Restoration Under Significant Additive Noise*", IEEE Signal Processing letters, vol. 14, No.6, pp.401- 404, (2007).
23. **R. L. Lagendijk, and J. Biemond,** " Basic Methods for Image Restoration and Identification", Academic press, (2000).
24. **A. Smirnov, and M. Ginzburg,** " *Iterative Image Restoration*"
http://www.cs.technion.ac.il/Labs/IsI/Project/Projects_done/VisionClasses/DIP/Iterative_Restoration/
25. **R. Gonzales, R. E. Wood , and S. L. Edding ,** " *Digital Image Processing Using Matlab* ", Prentice Hall,(2004).
26. **A. K. Kustsggelos, and M.G. Kang,** " *Iterative Evaluation of the Regularization Parameter in Regularized Image Restoration*", Journal of Visual Communication and Image Representation, vol.3 , No.4, pp. 446-459,(1995).
27. **J. Biemond, R. L. Lagendijk, and R. M. Mersereau,** " *Iterative Methods for Deblurring*", Proceedings of the IEEE, vol. 78, No.5, pp.856-883, (1990).
28. **S. Voloshynovskiy,** " *Iterative Image Restoration With Adaptive Regularization and Parametric Constraints*", Journal of Image Processing and Communication, vol. 3, 3-4, pp. 73-88, (1997).
29. **P. J. Verveer, and T. M. Jovin,** " *Acceleration of ICTM Image Restoration Algorithm*", Journal of Microscopy, vol. 188, pt3, pp. 191-195,(1997).
30. **K. G. Kang, and A. K. Kustsggelos,** " *Simultaneous Iterative Image Restoration and Evaluation of Regularization Parameter*", IEE Transaction on signal processing, vol. 40, No. 4, pp. 2329-2334, (1992).
31. **P. C. Hansen,** " *Digital Image Restoration*",
<http://www2.imm.dtu.dk/~pch/PPTSVD/pptsvd.html>
32. **H. C. Andrews and B. R. Hunt,** " *Digital Image Restoration*", Prentice Hall, Englewood Cliffs, N. J., (1977).
33. <http://www.lakii.com/vb/showthread.php?t=240961>

الخلاصة

ترميم الصور هي عملية نتيجة تقريبية لعمليات التدني وهي عملية معاكسة لعمليات التدني تقريباً لتقدير الصورة الأصلية وهي عمليات معاكسة لعمليات التدني تقريباً لتقدير الصورة الأصلية .

تقنية الترميم التكرارية ، المرشح المتبني (طريقة Tikhonov) صُمم لترميم صورة فضائية ملونة

مغوشة بضوضاء ثابت الفضاوي دالة النشر النقطية(دالة كاوس) ومشوشة بضجيج كاوس و Salt & Pepper بأختلاف معاملات التدني ، بعبارة أخرى بأختلاف نسبة الإشارة الى الضجيج وأختلاف كثافة الضجيج .

النتائج باستخدام المرشح المتبني قورن كميأ ، مع أنواع أخرى من تقنيات الترميم (مثل مرشح العكسي ، مرشح متوسط التريبعات الصغرى (مرشح فينر) ، مرشح بمعيار متوسط التريبعات الصغرى المقيدة) بأستخدام مربع معدل الخطأ ، النتائج أظهرت أن مربع معدل الخطأ لصورة مرممة يقل مع زيادة عدد تكرار العملية حتى النتيجة تقارب . كذلك النسبة لمربع معدل الخطأ لصورة متدنية الى صورة مرممة تزداد مع نقصان قيمة نسبة الإشارة الى الضجيج لضجيج كاوس وزيادة كثافة الضجيج ل Salt & Pepper بالترتيب .

النتائج أظهرت أن الطريقة المتبنية في البحث أحسن كفاءة لترميم الصورة المتدنية ، وخاصة لنسبة الإشارة الى الضجيج قليلة ، وكثافة الضجيج كبيرة .



جمهورية العراق
وزارة التعليم العالي والبحث العلمي
جامعة النهرين
كلية العلوم

ترميم الصور باستخدام تقنيات محورة غير خطية

رسالة

مقدمه الى كلية العلوم جامعة النهرين كجزء من متطلبات الحصول على
درجة ماجستير علوم في الفيزياء
من قبل

محمد خضير كاظم

(بكالوريوس ٢٠٠٥)

بأشراف

الاستاذ الدكتور أياذ عبد العزيز العاني

الاستاذ المساعد الدكتور صلاح عبد الحميد صالح

ربيع الثاني

١٤٢٩ هـ

حزيران

٢٠٠٨ م